AD_____

Award Number: W81XWH-12-1-0475

TITLE: An Injectable Method for Posterior Lateral Spine Fusion

PRINCIPAL INVESTIGATOR: Dr. Elizabeth Olmsted-Davis

CONTRACTING ORGANIZATION: Baylor College of Medicine
Houston, TX 77030-3498

REPORT DATE: September 2014

TYPE OF REPORT: Annual Report

PREPARED FOR: U.S. Army Medical Research and Materiel Command
Fort Detrick, Maryland 21702-5012

DISTRIBUTION STATEMENT: Approved for Public Release;
Distribution Unlimited

The views, opinions and/or findings contained in this report are those of the author(s) and should not be construed as an official Department of the Army position, policy or decision unless so designated by other documentation \

	Form Approved
REPORT DOCUMENTATION PAGE	*OMB No. 0704-0188*

1. REPORT DATE	2. REPORT TYPE	3. DATES COVERED
September 2014	Annual Report	1Sep2013-31Aug2014

4. TITLE AND SUBTITLE

An Injectable Method for Posterior Lateral Fusion

5a. CONTRACT NUMBER

5b. GRANT NUMBER
W81XWH-12-1-0475

5c. PROGRAM ELEMENT NUMBER

6. AUTHOR(S)
Dr. Elizabeth A. Olmsted-Davis

E-Mail: edavis@bcm.edu

5d. PROJECT NUMBER

5e. TASK NUMBER

5f. WORK UNIT NUMBER

7. PERFORMING ORGANIZATION NAME(S) AND ADDRESS(ES)
Baylor College of Medicine, Houston, TX 77030

8. PERFORMING ORGANIZATION REPORT NUMBER

9. SPONSORING / MONITORING AGENCY NAME(S) AND ADDRESS(ES)
U.S. Army Medical Research and Materiel Command
Fort Detrick, Maryland 21702-5012

10. SPONSOR/MONITOR'S ACRONYM(S)

11. SPONSOR/MONITOR'S REPORT NUMBER(S)

12. DISTRIBUTION / AVAILABILITY STATEMENT
Approved for Public Release; Distribution Unlimited

13. SUPPLEMENTARY NOTES

14. ABSTRACT
The central hypothesis of this application is that posterolateral spine fusion can be successfully achieved with a novel and simple minimally invasive percutaneous injection. We propose that this can be done by injection of AdBMP2 transduced human fibroblasts possessing an icasp9$_M$ that have been micro-encapsulated with osteoclast degradable hydrogel into the desired fusion site. During this first year, we have initiated the identification of the phenotype of the monocyte-like cells that appear to be capable of bone degradation. We have demonstrated in MSCs, which have a stably integrated icasp9$_M$, can be rapidly induced to undergo apoptosis, after delivery of a chemical inducer of dimerization (CID) after encapsulation in PEG hydrogel. The next step is to start *in vivo* testing of this system. Additionally we have developed the methodology to non-invasively locate the hydrogel microsphere placement, optically, with respect to the newly forming bone. This has lead to a publication. We have also initiated studies to fuse the spine using our cell based gene therapy system encapsulated in the PEG hydrogel microspheres, in both mouse and rat. We will continue to complete these studies in the upcoming year.

15. SUBJECT TERMS
BMP2, Spine fusion, PEG Hydrogel, Gene Therapy, Adenovirus.

16. SECURITY CLASSIFICATION OF:			17. LIMITATION OF ABSTRACT	18. NUMBER OF PAGES	19a. NAME OF RESPONSIBLE PERSON
a. REPORT	b. ABSTRACT	c. THIS PAGE			USAMRMC
U	U	U	UU	45	19b. TELEPHONE NUMBER *(include area code)*

Table of Contents

Page

INTRODUCTION: The treatment of many spinal problems involves stabilization of the spine by applying bone grafts to the posterior elements of the spine. The objective of these procedures is to induce bone to bridge between adjacent vertebral bodies and "fuse" the vertebrae into a larger bone mass. Posterolateral fusion of the spine is the most commonly performed of all the types of spine fusion and is useful for the treatment of scoliosis, instability and painful degenerative conditions of the spine. We recently demonstrated that adenovirus transduced cells expressing BMP2, when injected into the paraspinous musculature, could rapidly form new bone at the targeted location and efficiently fuse vertebral bone at a desired site, within 2 weeks. Encapsulation of these cells in poly(ethylene glycol)-diacrylate (PEGDA) hydrogels allowed for longer survival of the cells *in vivo*, did not result in inflammation, which otherwise completely ablate new bone formation/fusion, and maintained the cells at the target location. Thus our preliminary data demonstrates the ability to induce new bone formation at the desired fusion location without need for any surgical intervention. Here we propose to engineer additional safety features into the material by using an inducible caspase 9 ($icasp9_M$), which when activated will induce apoptosis within the transduced cells. Further, the hydrogel will also possess an osteoclast selective protease site which allows for removal of the biomaterial during bone remodeling.

KEYWORDS: BMP2, claudin 5^+ progenitors, de novo bone formation, osteoprogenitors

OVERALL PROJECT SUMMARY: ***Task 1: To characterize the ability of the molecular therapy system to rapidly induce fusion of the new bone with the vertebra, through induction of osteoclast progenitors (OCP) – monocyte progenitors.*** The proposed studies in this aim are an extension from our previous findings that monocyte-like cells that are not multinucleated osteoclasts were observed at the fusion site between the new heterotopic bone, and skeletal bone (figure 1). These cells appeared to be contributing to the remodeling

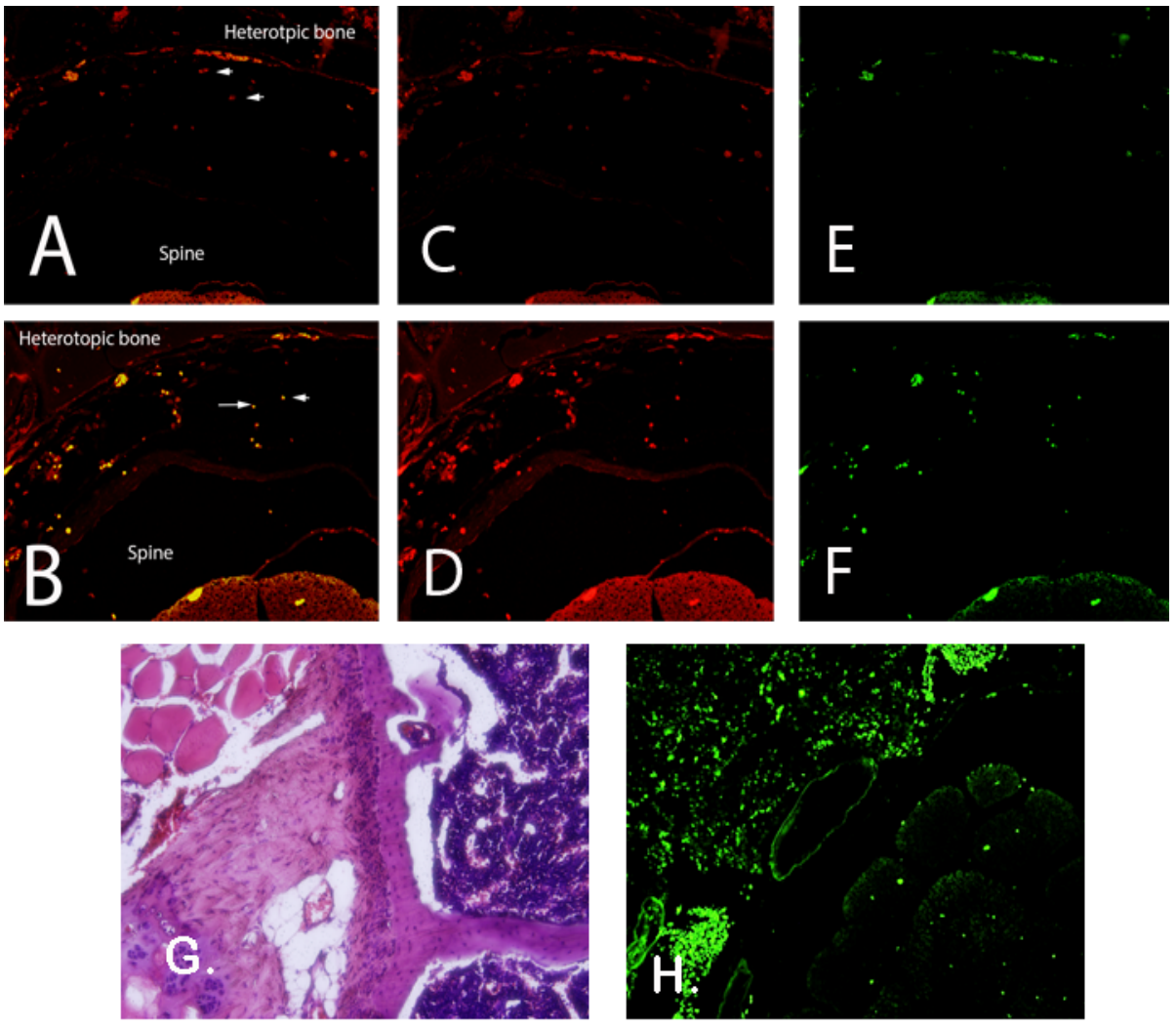

Figure 1: Representative photomicrographs of tentative vertebral fusion with the heterotopic bone. The slides were immunostained for **(A and C)** CD11b (red), **(A and E)** fractalkine (green) and merged in **(A)**. In panels **(B and D)** fractalkine (red), **(B and E)** LyC6 (green), and **(G)** hematoxylin and eosin for viewing. Panel H depicts a nerve with positive staining for LyC6 in the perineurium. These are representative photomicrograph (10X) of a sample taken 4 weeks after the initial injection of AdBMP2 transduced cells.

of the fusion structure, and may be critical to enhancing fusion between the two bones. We propose that if we could characterize and isolate these cells, they may be beneficial in enhancing spine fusion, in other model systems as well as our own. One of the first steps is to determine their phenotype and determine if they are actually specialized M2 macrophages expanded to aid in matrix remodeling and fusion.

Therefore we have secured animal approval for the studies, and performed spine fusion in mice to generate tissue sections for initial phenotypic characterization of these spines. In these experiments, mice (n= 4) were injected with AdBMP2 or Adempty transduced cells and then spines isolated at weekly intervals (1-6 weeks) and serial sections generated, that represent the fusion process in the animals. We then initiated immunohistochemical staining with key antibodies that will be used for fluorescence activated cell sorting (FACs). These antibodies (CD11b ^{lo}, fractalkine^{+}, Ly6C^{+}), are surface antigens that can readily allow us to sort populations of cells for testing in bone resorption assays. After initial optimization of the antibodies, we observed co-localization of fractalkine^{+} and Ly6C^{+} in the cells, but as expected they were not expressing CD11b (figure 1). These cells were found lining the junction between the heterotopic bone and the new bone (figure 1, panel B). What was further intriguing was that cells associated with the perineurium of the nerve were also LyC6^{+} but not fractalkine^{+}. It is unclear whether these cells may function as an earlier progenitor, or whether they are just a separate population. We will continue to characterize this phenptype.

The next step is to isolate and further characterize the phenotype of these cells specifically to demonstrate their potential M2 nature. Also we will collect the various positive and negative populations and confirm their bone resorption ability using a standard assay kit (Bone Resorption Assay Kit; CosmoBio Co, Ltd) that uses a fluoresceinated calcium phosphate-coated plate. Additionally, we will isolate and test these cells *in vitro* to determine whether they respond to Lipopolysaccharide (LPS) and the proinflammatory cytokine interferon-γ (IFNγ) to promote a classically activated M1 macrophage expressing IL-12 or conversely if exposure to IL-4 or IL-13 will promote an "alternatively activated" M2 phenotype that expresses IL-10. We predict that those studies will be completed within the next year.

Task 2: To increase the safety and controllability of the procedure through selective ablation of the cellular component of the microspheres followed by osteoclast specific resorption on the polymer, and bone healing.

We first wanted to introduce and inducible caspase 9 (icasp9$_M$) into the delivery cells so that the BMP2 production could be regulated by systemic delivery of a chemical inducer of dimerization (CID). This in turn would cause the icasp9$_M$ to become activated and initiate an apoptotic pathway leading to cell death. Therefore we generated human mesenchymal stem cells that possess a stably integrated icasp9$_M$ as well as a GFP reporter. We also obtained an MSC cell line that does not possess the icasp9$_M$ for use as an additional control. In these first experiments we determined the timing of cell death (figure 2) and determined whether this would attenuate the BMP2 expression (figure 3). We observed immediate killing of the cells greater than 95% after exposure to the CID, however, the vehicle did not lead to any significant cell death. We next looked at BMP2 expression after deliver of a single dose of CID on day 1 (figure 3). BMP2 activity was assessed through an assay in which the bone marrow cell line W20-17 will undergo osteogenic differentiation, and up regulate alkaline phosphatase activity, in the presence of active BMP2. The results suggest

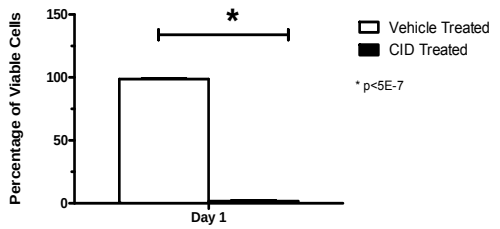

Figure 2: Cell death was immediate following delivery of the 0.1 nM chemical inducer of dimerization (CID)

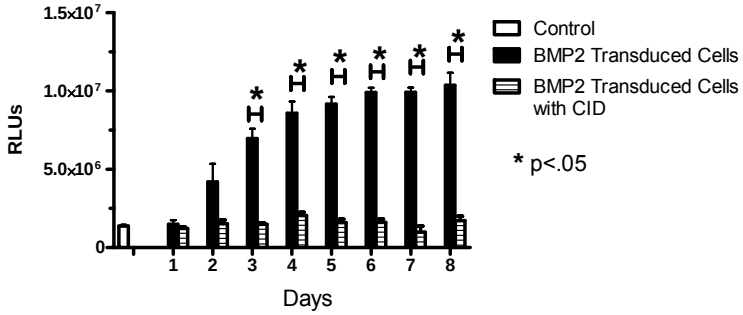

Figure 3: BMP2 activity in the presence and absence of CID. W20-17 cells were exposed for 3 days with media isolated from MSCs + icasp9$_M$ transduced with AdBMP2 (5000vp/cell) and in the presence of absence of CID. The CID was delivered on day 1, and remained in the cultures, throughout the assay.

that the single dose of CID was able to ablate the expression of BMP2 in the cells, but the cells were capable of being efficiently transduced to produce active BMP2.

We next attempted to encapsulate the cells and determine if they were capable of producing BMP2 to confirm that the CID would freely diffuse into the hydrogel, and activate the icasp9$_M$ similarly to the unencapsulated cells. As seen in figure 4, although the preliminary data appears to be variable, the encapsulated cells appear to produce similar amounts of the BMP2 as the unencapsulated cells. We next looked at the ability of the encapsulated cells to undergo apoptosis in the presence of CID (figure 5A and B). These preliminary experiments suggested that within 24 hours approximately 60-75% of the cells were observed expressing the dsRED in the MSCs + icasp9$_M$, but was reduced to approximately 40% of the cells expressing the dsRED after delivery of the 0.1nM CID. Alternatively, approximately 80% were observed expressing the dsRED in the control MSCs lacking the inducible caspase 9 regardless of the presence of CID. Although preliminary these studies suggest that the CID is able to induce apoptosis in the encapsulated cells. Further studies are ongoing to follow up and optimize the kinetics and delivery of CID to the encapsulated cells.

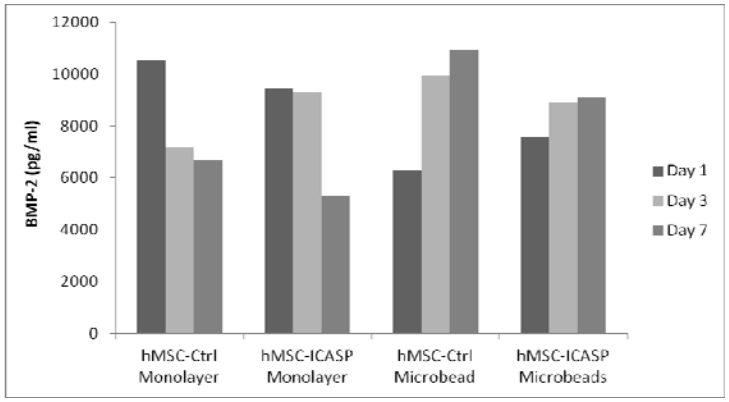

Figure 4. Comparison of BMP2 secretion in the monolayer versus the encapsulated cells.

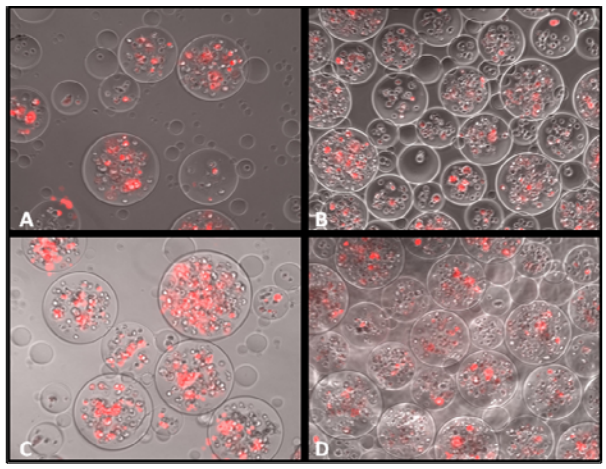

Figure 5A: Comparison of dsRED expression in MSCs or MSCs + icasp9$_M$ in the presence of CID. Cells were transduced with AddsRED (5000vp/cell) and cell death was scored as the absence of red color. **(A)** hMSC-Ctrl w/o CID; **(B)** ICASP w/o CID; **(C)** hMSC-Ctrl w/ CID; **(D)** hMSC-ICASP w/ CID.

Control MSCs	**Samples with HO**
No CID	100%
CID delivered on day 1	50%
CID delivered on day 4	75%
CID delivered on day 11	50%
icasp9$_M$ MSCs	
No CID	100%
CID delivered on day 1	25%
CID delivered on day 4	25%
CID delivered on day 11	75%

Table 1: Preliminary analysis of the HO in the presence or absence of CID in MSCs and MSCs + icasp9$_M$

We also performed a very preliminary study to look at whether delivery of the CID could then suppress bone formation *in vivo*. In these studies, the MSCs or MSCs + icasp9$_M$ were transduced with AdBMP2 (5000vp/cell) and then injected into the rear hind-limb of NOD/Scid mice. Bone formation was detected using x-ray approximately 15 days after the initial injection (figure 6). Although there was significant variability within groups (Table 1), the trends suggest that deliver of the CID was able to

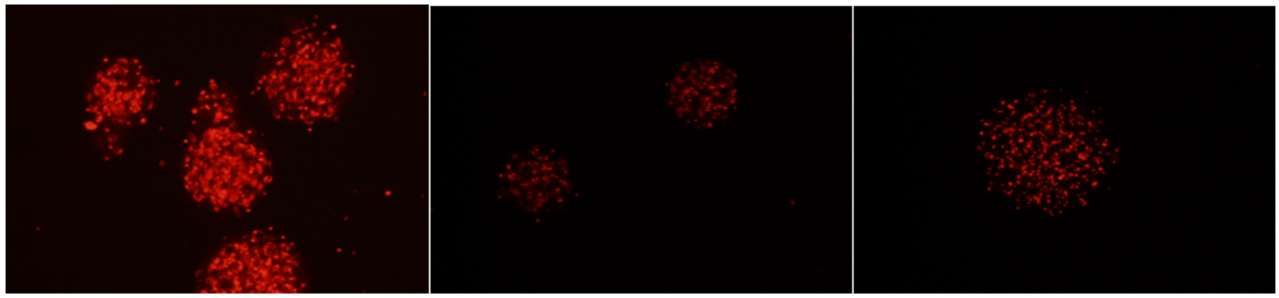

Figure 5B: Comparison of dsRED expression in PEGDAencapsulated MSCs-icasp psossessing a dsRED reporter 24 hours after exposure to **(A)** vehicle **(B)** CID and **(C)** polyethylenimine (PEI) cytotoxin.

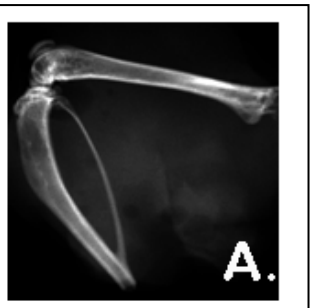

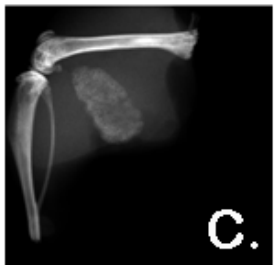

Figure 6: Radiological evaluation of bone formation 15 days after animals received AdBMP2 transduced MSCs + icasp9$_M$ followed by systemic delivery of CID **(A)** day 1, or

suppress the bone formation when delivered earlier in the reaction (figure 6, panels A and B). However, when delivered at 11 days after initial induction of HO, the majority of the samples had significant HO (figure 6, panel C). We are currently repeating a many of these experiments to gain optimize the CID dose, and delivery time, with enough replicates to afford statistical analysis and publication. We are currently assembling a manuscript to describe these experiments and we predict this will be completed within the next 3 months. Additionally we will initiate similar experiments in the GPSG or degradable hydrogel microspheres.

This year we have also been focused on further characterizing the GPSG hyrogel microspheres *in vivo* in mice to determine the resorption kinetics of the materials. The cells are transduced with AdRiFP and AdBMP2 and encpasulated in either the PEGDA hydrogel or the GPSG microspheres containing an Alexafluor dye. Then the mice are transferred to the Dr. Sevick's laboratory for imaging of both the termination of the RiFP and Alexafluor reporters. These can be individually visualized by Dr. Sevick's group (Lu Y, *et al,* 2013) and this allows us to watch both termination of the cells and degradation of the polymer *in vivo*. We originally proposed to perform these experiments in rat; however, we are requesting that we be able to continue with mice since we are not able to obtain reliable *de novo* bone formation (see next section).

Task 3: To assess and compare bone quality of the skeletal and new bone during and after completion of the fusion.

To accomplish this, we have developed a non-invasive optical imaging methodology to determine the optimal dose of microspheres with respect to their placement, cell viability and resultant bone formation. Therefore we altered our approach by incorporating an Alexafluor dye into the PEG hydrogel that could be detected optically. To further confirm viability of the cells, we transduced the cells with AdIFP and AdBMP2, so that we could follow the cells. Initial experiments were performed to then detect the presence of the two reporters with respect to the newly forming bone. Since this involved both optical imaging and co-alignment with microCT, we had to develop novel methodology to integrate the systems. These experiments lead to a publication of this methodology (see appendix). **We have been unable to reliably obtain de novo bone formation at a targeted site in the wild type rats. This has prevented us from moving forward on looking at spine fusion.** However, we did note that enhancement of orthotopic bone formation and fracture repair was able to work very well with this system (Sonnet C. *et al*, 2012). We next attempted to determine why the rat was unable to make *de novo* bone at all sites. Since we knew that we could make orthotopic bone at a fracture site, we next attempted to induce *de novo* bone at a site very close to the intact skeletal bone and compared this to bone formation when the same cells were injected into the hind limb at a site distal from the skeletal bone, but still placed in the muscle and adipose (figure 7). To achieve this type of injection, mice were x-rayed with the syringe placed, to ensure that they were not touching the skeletal bone and that placement was as reported. Surprisingly, we observed robust bone formation as determined by radiological and histological analysis, but at the site close to the skeletal bone, but did not observe bone formation at the distal site (figure 8). We observed no differences in the bone formation when we injected in both legs of one animal or whether we used different rats for a single injection. However, if we were to inject both distal and close in the same leg, then we observed two distinct regions of bone formation. We confirmed by histological analysis that the bone formation was distinct from one

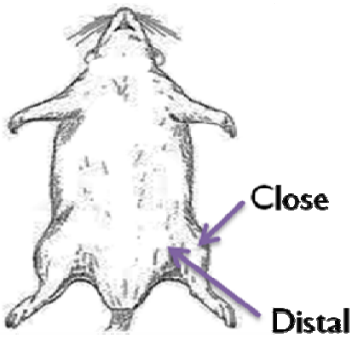

Figure 7: Schematic of the location were microbead encapsulated cells were injected into the rat hindlimb

another, rat hind-limb tissues were into formalin fixed, decalicified and cut into two separate pieces for sectioning. Tissues were then parffin embedded, and serially sectioned through the bone reaction site for each piece. We located the reaction site, through hematoxylin and eosin staining of every 5th slide. The distal appearing in block A, while the close in block B. There appeared to be normal muscle tissue separating the two reactions sites. The bone formation appeared to be significant at both locations. Further, in the tissues receiving the distal injections alone, we identified the reaction site through localizing the nondegradable microspheres, but we did not observe any bone. Further, the bone by microCT in all cases of the close injection appeared to be distinct from the skeletal bone. However upon histological analysis we did observe in many cases what appeared to be a cellular structure that ultimately connected back to either the fibula or tibia skeletal bone. In all cases a control was also included which was Adempty cassette transduced cells microencapsulated in PEGDA hydrogel. These cells also did not encite new bone formation as determined by histological analysis. The data collectively suggested that perhaps cells were migrating from the periosteum, or that in the close injection the periosteum was reacting to the BMP2 to form bone whereas in the distal injection the periosteum was too far from the BMP2 being secreted therefore the reaction was unable to progress. Alternatively it another possibility may be that the periosteal cells are unable to migrate beyond a specific distance. In either case, the results are very different from those in the mouse where we previously showed that peripheral nerves were the source of progenitors for *de novo* bone formation (Salisbury *et al*, 2012 and Lazard *et al*, 2014 in Review see appendix).

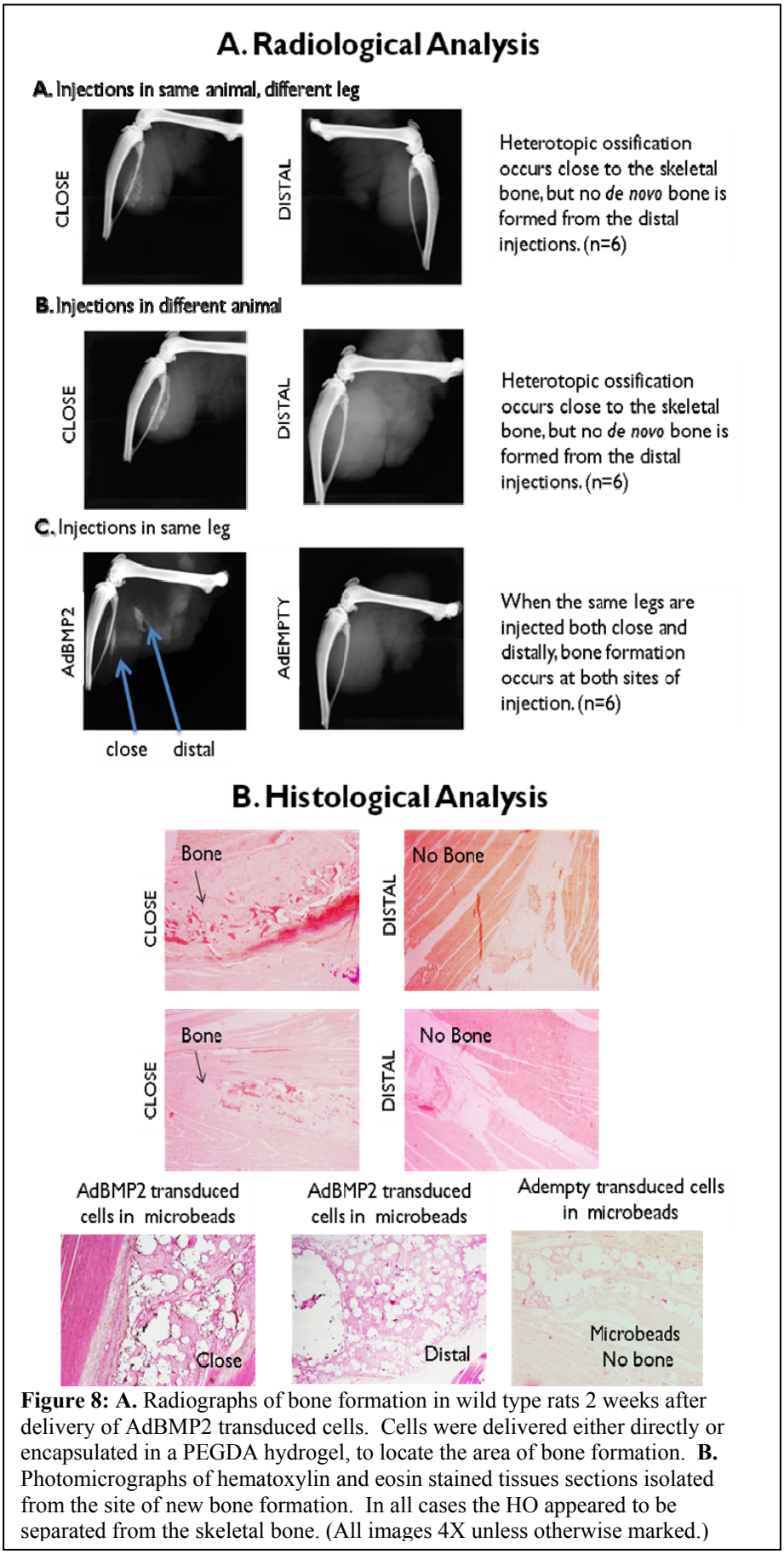

Figure 8: A. Radiographs of bone formation in wild type rats 2 weeks after delivery of AdBMP2 transduced cells. Cells were delivered either directly or encapsulated in a PEGDA hydrogel, to locate the area of bone formation. **B.** Photomicrographs of hematoxylin and eosin stained tissues sections isolated from the site of new bone formation. In all cases the HO appeared to be separated from the skeletal bone. (All images 4X unless otherwise marked.)

To confirm whether periosteal cells were contributing as a source of osteoprogenitors, and compare the process found in mice to that in the rat, we next isolated tissues that had undergo *de novo* bone formation through injection of the AdBMP2 cells at the close site to ensure bone formation. In these studies, the tissues were isolated and analyzed on days 2, 4, 6, and 8 after delivery of the AdBMP2. By day 10 we observed mineralized bone by x-ray (data not shown). Tisues again were serially sectioned and the reaction area identified by H& E staining of every 5th slide. Once the area of interest was located, the unstainned serial sections remaining in this region were subject to immunohistochemistry. Figure 9 shows representative photomicrographs of both the hematoxylin and eosin stained tissues (H & E) as well as the tissues immunostained for various markers of either the osteoprogenitor (Claudin 5, PDGFRα, osterix), transient brown adipose (UCP1), blood vasculature (CD31 also known as PECAM) and periosteum (Periostin). Also to confirm the

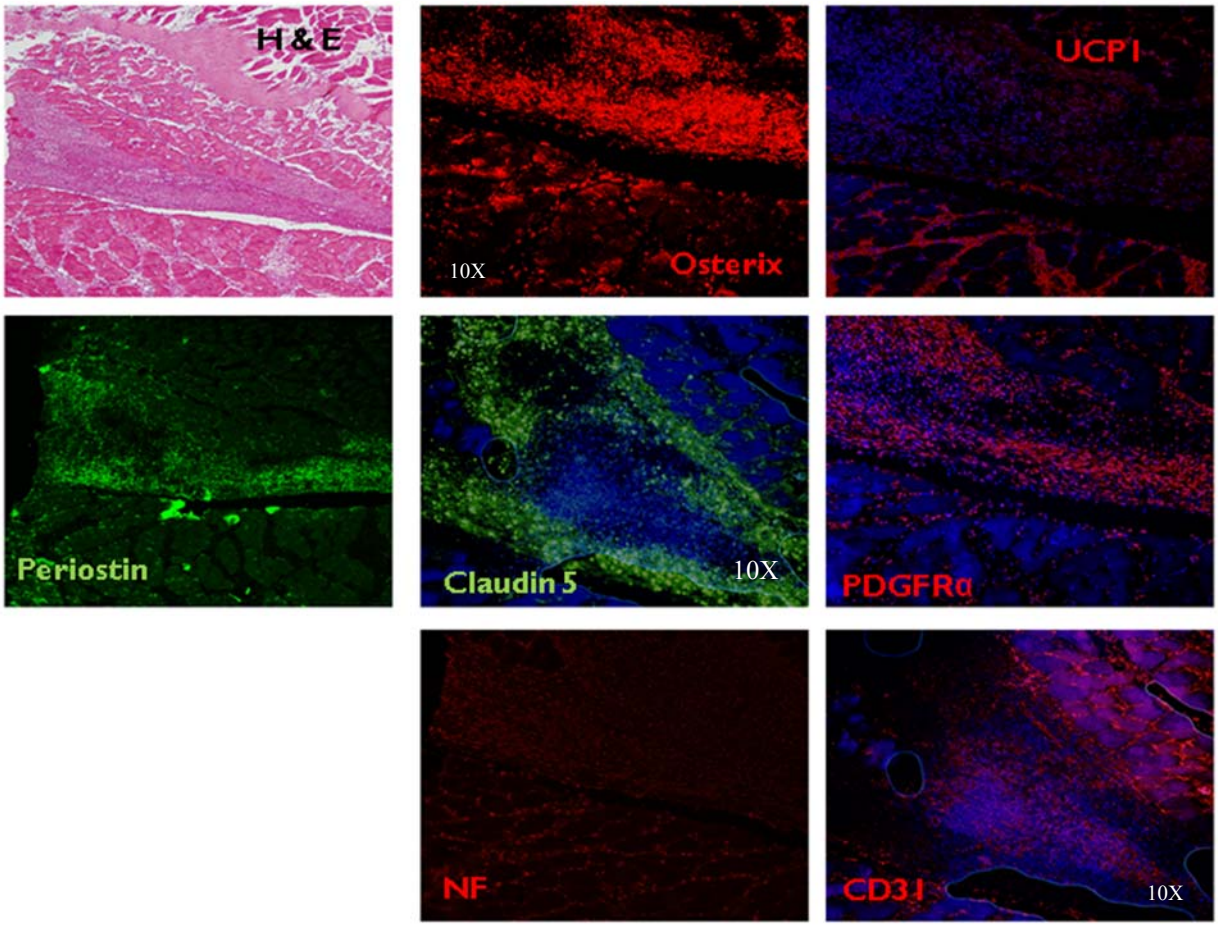

Figure 9: Claudin 5-PDGFRα osteoprogenitors appear to migrate from the periosteum of skeletal bone towards the BMP2 producing cells as early as 2 days after induction of bone formation. Representative, photomicrographs of immunohistochemical staining on serial paraffin decalcified sections generated from the entire rat hind limb 2 days after the delivery of AdBMP2 transduced cells. Antibodies were selected based on the mechanisms in mouse which suggest the osteoprogenitors are claudin 5^{+} PDGFRα^{+} cells and that UCP1^{+} brown adipocytes play a key role in bone formation. (All images 4X magnification unless otherwise specified).

location of larger nerves we immunostained with neurofilament (NF) that does not detect the periosteum. This allowed us to confirm whether the nerves or the periosteum were responding to the BMP2. The data suggests that the osterix^{+} cells possessing similar markers (PDGFR$\alpha^{+}$and claudin 5^{+}) to those coming from the endoneurium of the nerve in mice appeared to be migrating towards the site of the AdBMP2 transduced cells (figure 9 and appendix). To locate the delivery cells, human cells were used to deliver the BMP2 that can readily be detected by a specific human mitochondrial antibody - data not shown). These tentative osteorprogenitors are also expressing osterix similar to the endoneurial derived cells in the mouse (see appendix), however, these cells also express periostin and appear to be derived from the periosteum lining the skeletal bone. Interestingly, UCP1^{+} transient brown adipocyte-like cells were also found co-localizing, but nonoverlapping with the tentative osteoprogenitors similar to in the mouse (fig 9). We observed a large number of small vessels near the periosteum, but if was impossible to note whether these were changing, and comparison with a control, suggested that they were pre-existing in this location. Interesting, large nerves were identified near the reaction area, but at this time point were not positive for any of the markers beyond NF (figure 12).

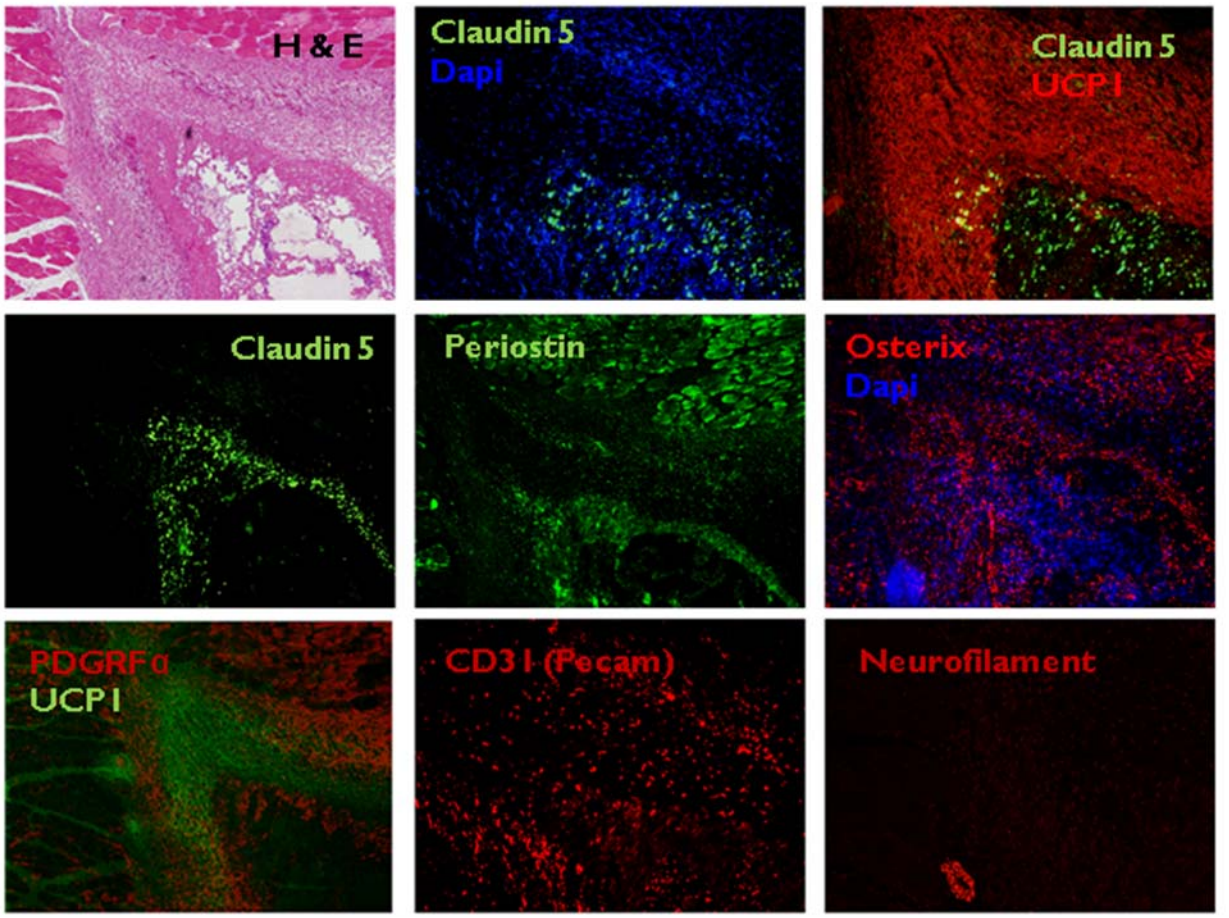

Figure 10: Claudin 5-PDGFRα osteoprogenitors appear to migrate from the periosteum of skeletal bone towards the BMP2 producing cells as early as 4 days after induction of bone formation. Representative, photomicrographs of immunohistochemical staining on serial sections generated from the entire rat hind limb 4 days after the delivery of AdBMP2 transduced cells. Antibodies were selected based on the mechanisms in mouse which suggest the osteoprogenitors are claudin 5^{+} PDGFRα^{+} cells and that UCP1^{+} brown adipocytes play a key role in bone formation. 10X magnification

Analysis of tissues isolated 4 days later, showed similar patterns as the tissues from day 2 however, now the reaction-periosteal cells have migrated a much larger distance from the skeletal periosteum. The periostin staining in figure 10 shows complete overlap with claudin 5^{+} PDGFR^{+} cells, but these cells connect back to the periosteal structure only at some points by a single cell layer. The massive foci of positive staining appear to be establishing the pattern of *de novo* bone. Again interestingly, the UCP1^{+} cells are co-localized with the osteoprogenitors, and presumably serve a necessary functional role. Again there are a number of vessels in this

region, and studies are ongoing to determine if these are newly synthesized to support the new bone or pre-existing. This is an important aspect since in the mouse large numbers are newly synthesized to support the extravastion of the tentative osteoprogenitors that circulate from the nerve to the site of *de novo* bone (see apenndix). Similar findings were observed in tissues isolated 6 days after the induction by delivery of AdBMP2 transduced cells. In these studies, newly synthesized cartilage can just start to be observed on the hematoxylin and eosin stainned slide (figure 11). Interestingly, all the same markers persist on the tentative osteoprogenitors which sit in the region near the new cartilage. Further the transient brown adipocyte-like cells continue to co-localize to this region but do not overlap the other markers, supporting our theory that they have a key functional role in regulating oxygen tension within the tissues necessary for cartilage development. Additionally it is fascinating to note that the progenitors have been at the location of bone formation prior to the appearance of cartilage suggesting that these processes do not couple as in normal skeletal bone. The data collectively suggests that the rat utilizes similar processes but recruits the precursors from the periosteum rather than peripheral nerves.

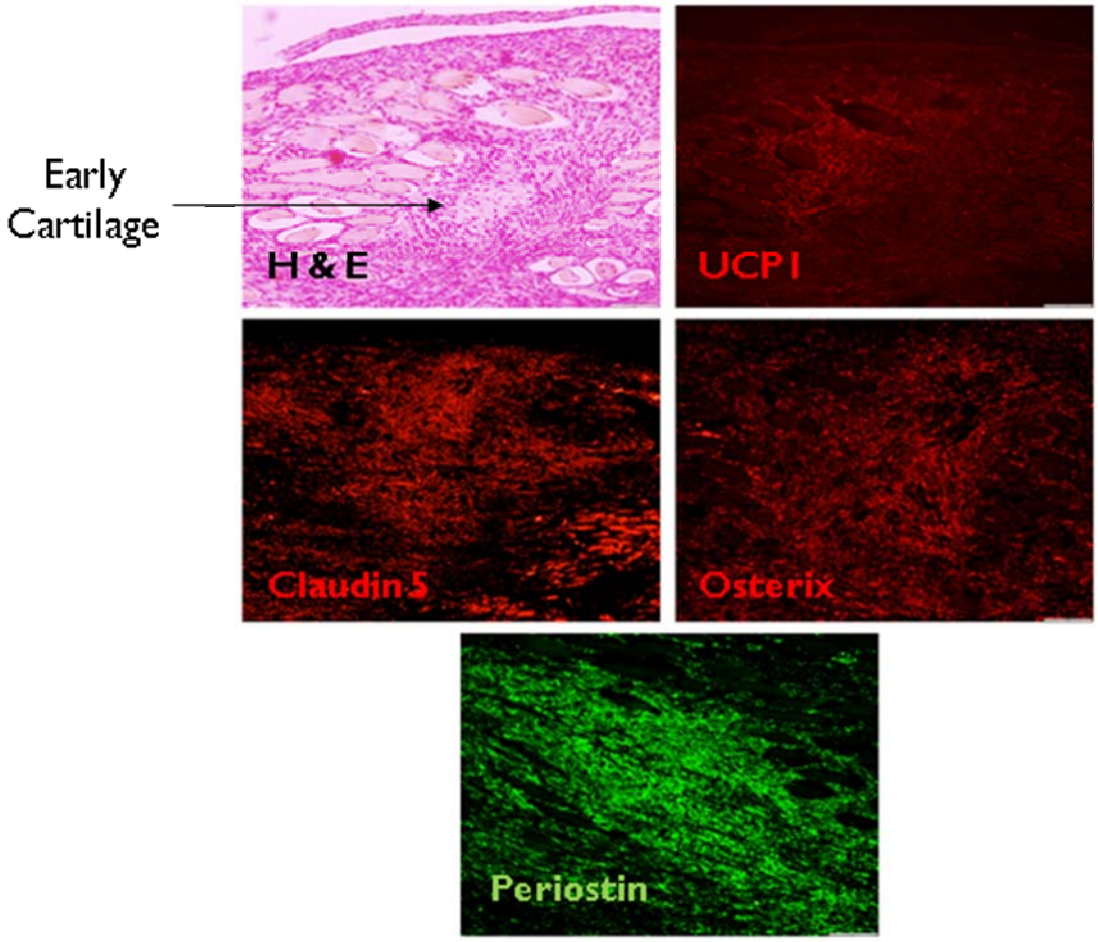

Figure 11: Claudin 5-PDGFRα osteoprogenitors appear to migrate from the periosteum of skeletal bone towards the BMP2 producing cells as early as 6days after induction of bone formation. Representative, photomicrographs of immunohistochemical staining on serial sections generated from the entire rat hind limb 4 days after the delivery of AdBMP2 transduced cells. Antibodies were selected based on the mechanisms in mouse which suggest the osteoprogenitors are claudin 5^+ PDGFRα^+ cells and that UCP1^+ brown adipocytes play a key role in bone formation. 10X magnification

To better determine why the peripheral nerves do not appear to be responding, we focused directly on whether they contained similar precursors as in the mouse. Interestingly, we observed the cells in the endoneurium compartment of the mouse nerve only on the first day, and then after ward the cells appeared to circulate (appendix). In all subsequent days after the first 24 hours the cell were absent in the nerve (figure 12). Similarly, we did not observe the cells on the nerves within the site of *de novo* bone formation at 2 days after induction, but by day 6 we observed a significant number of cells within the nerves (figure 12). In fact these nerves were extremely positive for claudin 5, wherease at a similar time frame in the mouse they were completely negative (see appendix). Previous studies in the mouse have shown that there is an osteoprogenitor that will build up on the nerve and fail to migrate in the presence of cromolyn (Salisbury E. *et al*, 2011 and appendix). Cromlyn blocked mast cell degranulation, and activation of MMP9, preventing the migration of the

perineurial progenitors and formation of tBAT (Salisbury *et al*, 2012). We hypothesize that the building up of osterix^{+} cells within the endoneurium is due in part to the contribution of

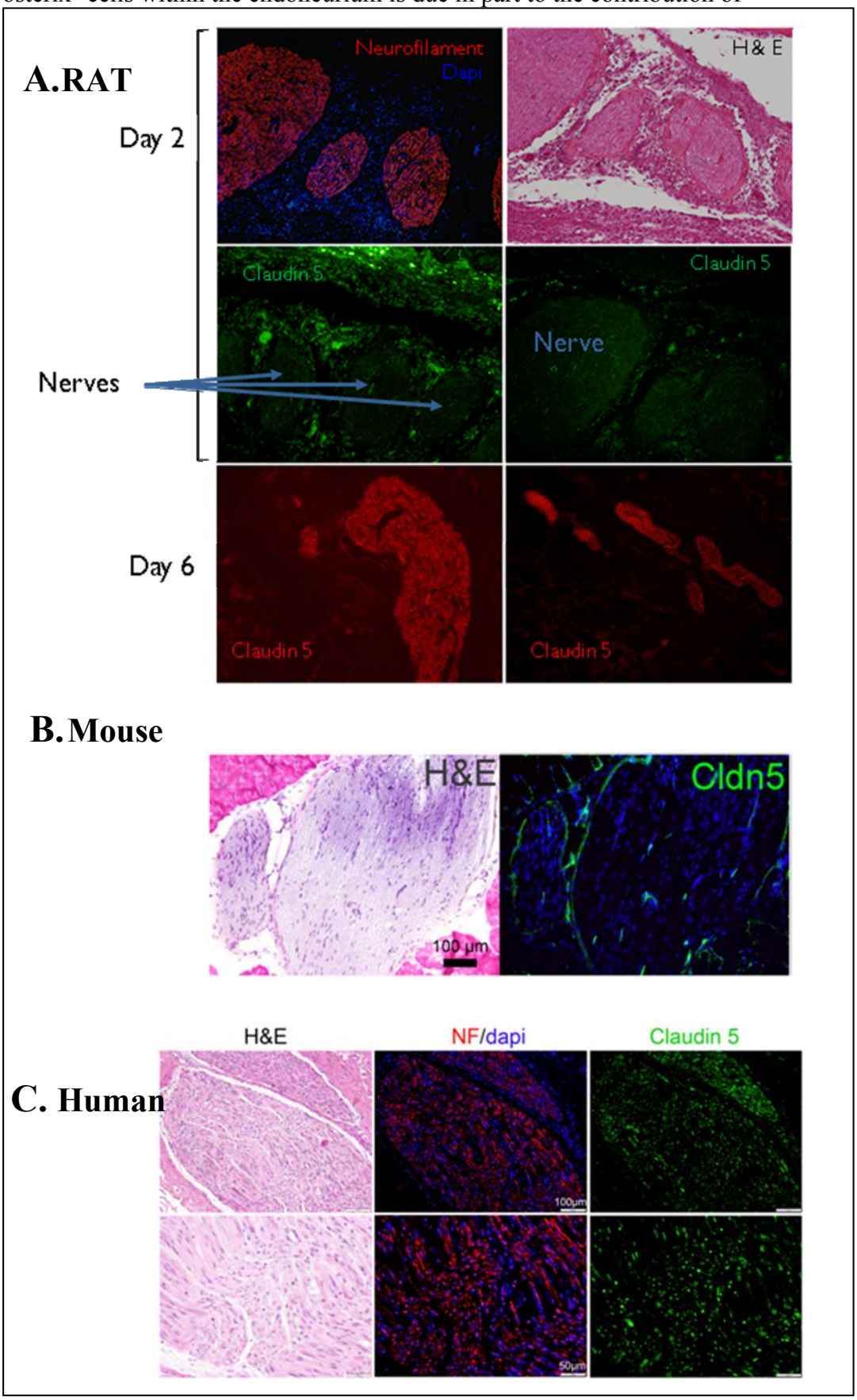

Figure 12: Claudin 5 expression in the nerves of mouse, rat and human. Photomicrographs of immunohistochemical staining on serial paraffin decalcified sections generated from **A.)** rat days 2 and 6 and **B.)** mouse hind limb 2 days after the delivery of AdBMP2 transduced cells. (All images 10X magnification). **C.)** Human sections were obtained from heterotopic ossification in an amputation stump and may vary in maturity

perineurial cells to the tight junction within the endoneurium that governs exiting of the cells. We propose that the perineurial cells remain unchanged blocking the ability of the cells to exit into the circulation when in the

presence of cromolyn. However, in normal cases the cells exit and do not come back (see appendix and figure 12). Interesting, human tissues obtained through an approved IRB protocol, using funds not associated with this application, revealed nerves that were also positive for claudin 5; however, these were taken from an amputation stump, and may be invoved in neuroma formation. Reports suggest that both the perineurial cells and endoneurial cells expand in nerves at the amputation site, in response to the injury to form neuroma. Therefore the inability for the progenitors to exit the nerve may be an additional abherrant process. We are currently looking at MMP9 expression which is activated within 24 hours of delivery of the BMP2 and resides along the perineurium of peripheral nerves at the site of bone formation in the mouse model (Rodenberg E *et al*, 2011). Figure 13 shows a schematic of the two models of bone formation and how they differ. We propose to characterize the expression of MMP9 in these same tissues to determine if that may be the breakdown. Further, we will quantify the presence of mast cells within the nerves located within the region of bone formation, to determine if there is a higher number of cells as observed in the mouse model (Salisbury E. *et al*, 2012). We propose that if the nerve is unable to be remodeled immediately after delivery of the AdBMP2 producing cells, then bone formation may be hampered or ablated, depending on whether the periosteum can be used as an alternative site. Further, we propose that the *de novo* bone formation to fuse the spine in the rat does not occur due to the lack of responsive periosteum on the vertebral bone.

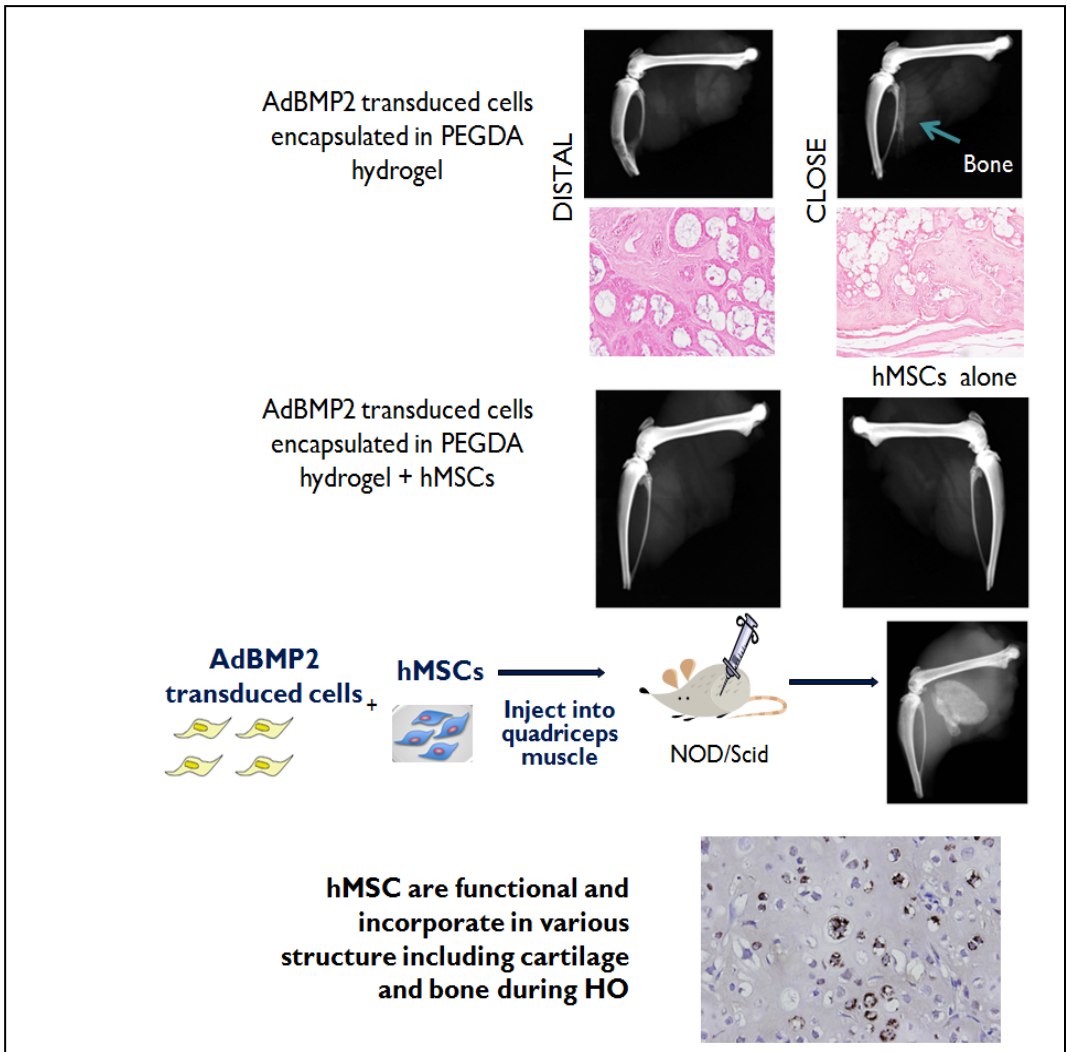

Figure 13: Human MSCs were co-injected with AdBMP2 transduced cells at a distal location into a rat hind limb muscle. Tissue was isolated 2 weeks after injection and subject to radiological and histological analysis. Histology confirmed the radiographs that bone formed when close to skeletal bone, but not with the distal injection. Further, hMSCs failed to rescue the bone formation, although these same cells readily incorporated into bone and cartilage associated with HO in mice.

If the periosteum is the only source for precursors and that there is a critical distance by which they can be recruited to travel and contribute to *de novo* bone formation, then we hypothesize that providing progenitors would rescue the bone formation at the distal location. Since the standard for osteogenic progenitors is a bone marrow mesenchymal stem cell we next obtained these cells (*gift from Dr. Carlos Ramos, M.D. BCM-CAGT*) and tested these to see if they would rescue the *de novo* bone formation when injected at a distal location. In these experiments athymic rats were injected distally with either AdBMP2 transduced cells alone, close (postive control) or distal (negative control) or in combination with 1

million hMSCs (fig 13). A similar number of hMSCs were injected without the AdBMP2 transduced cells (fig 13). Further, to confirm that the phenotype of the cells was perserved so that they were capable of undergoing differentiation into the various mesenchymal structures such as bone, cartilage, adipose etc, a subset of the hMSCS were also injected into a NOD/Scid mouse, along with AdBMP2 transduced cells, to drive engraftment of the cells (fig 13). Radiolographic images suggested that the hMCS alone did not induce *de novo* bone formation nor did they rescue bone when injected with the AdBMP2 cells at the distal location. However the AdBMP2 transduced cells were capable of launching *de novo* bone formation when injected at a close proximity to the skeleton (fig 13). Further, the hMSCs did robustly engraft into cartilage, bone and adipose structures in the mice undergoing rapid bone formation as determined by visualizing the cells within the newly forming tissues by using an antibody specific for human cells (fig 13). The data suggests that the hMSCs could undergo chondro-osseous differentiation, but were incapable of inducing bone either by themselves or but also they could not function as osteoprogenitors in *de novo* bone formation induced by delivery of the AdBMP2 transduced cells. This was surprising but suggests that they may not be capable of functioning as a chondro-osseous progenitor in this system.

We next looked isolated decided to isolate periosteum from rats either untreated or from rats that received a close injection of AdBMP2 transduced cells two days prior to harvesting. The periosteum was

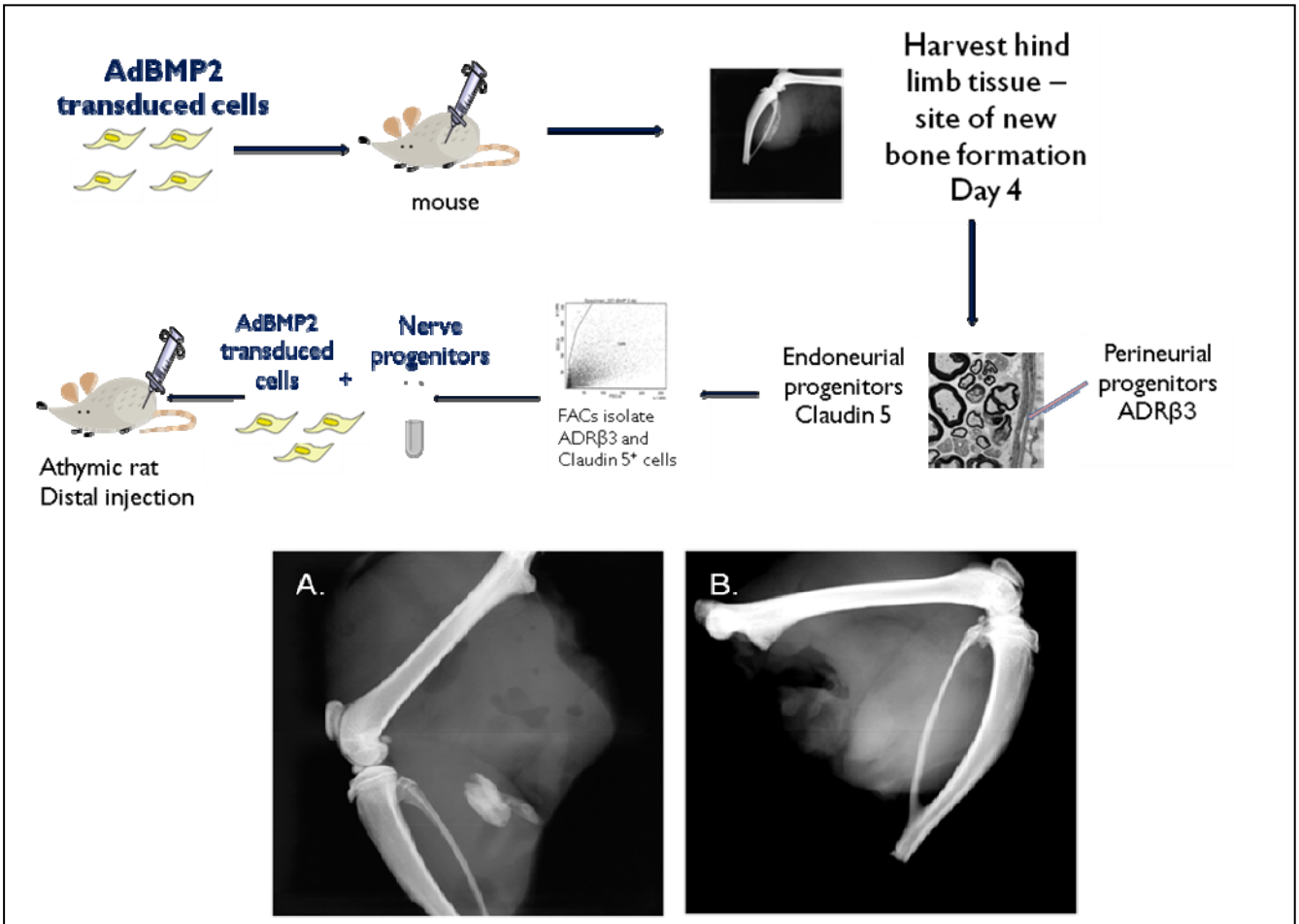

Figure 14: A schematic of the experimental plan and resultant radiograph of AdBMP2 transduced cells co-injected with the isolated mouse nerve progenitors. Mouse ADRβ3^{+} and claudin 5^{+} cells isolated 4 days after induction of de novo bone formation by BMP2. Presumably this allowed for their expansion and recruitment to the location of bone formation. However, at this stage the mouse tissues had no detectable cartilage or bone. The cells were isolated by FACS and then **(A.)** combine with AdBMP2 transduced cells or **(B.)** AdBMP2 transduced cells were injected alone. Bone formation was measured in the rats approximately 2 weeks later. (n=2)

removed from the long bone and digested briefly with collagenase then extensively washed with PBS and resuspended (1 million cells) in the syringe along with the AdBMP2 transduced cells, and then again injected at a distal location to see if they would rescue the *de novo* bone formation. Interestingly, we did not observe rescue of the bone formation in the hind-limb or bone formation (Data not shown). One problem is that the preparation

of cells was a crude preparation, and we were unable to determine if the progenitors still remained in the periosteum, and if they were in the final isolated cell population. Therefore we next isolated the claudin 5^+ population from C57BL/6GFP mouse tissues 4 days after receiving the AdBMP2 transduced cells through cell sorting. We also isolated simultaneously the ADR$\beta 3^+$ cells (this is the UCP1^+ population Salisbury *et al,* 2012), which is the other cell population in mice that is derived from peripheral nerves 4 days after induction of *de novo* bone formation. These two populations of nerve derived progenitors were pooled and 1 million cells were co-injected with the AdBMP2 transduced cells at the distal location in the rat hind limb. The radiolographic analysis suggested that these progenitors could rescue the bone formation (fig 14). However, we are currently completing these experiments, to determine whether the newly formed bone is comprised of rat cells or C57BL/6GFP mouse cells. Further, we will confirm whether these cells were capable of making bone in the abesence of AdBMP2 in the rat. Upon completion of these experiments, we will attempt to rescue spine fusion in the rat using these cells. If successful, we will then attempt to include the microbeads, both GPSG and PEGDA formulations in a rat model of spine fusion. However in the interim, we will continue to develop them biomaterials in a mouse model, rather than rat, so as not to impede our progress towards the deliverables.

KEY RESEARCH ACCOMPLISHMENTS: We have:

- Approval of animal experiments
- Initiated characterization of monocyte-like cells
- Obtained stable MSC cell lines possessing the inducible caspase 9 ($icasp9_M$)
- Demonstrated the ability of these cells to secrete BMP2 after transduction with adenovirus
- Shown that these cells are viable after encapsulation
- Shown that these cells respond to the CID (or activator of apoptosis) by undergoing cell death, and through the lack of BMP2 within the culture supernatant
- Started to characterize the optimal dose of the CID to induce similar rapid cell death and suppression of the BMP2
- Started to characterize the kinetics of in vivo delivery of CID, and resultant suppression of bone formation.
- Developed methodology for optical detection of integrated near infrared reporters in the hydrogel microspheres
- Developed methodology for co-localizing the optical data with microCT data of resulting bone formation.
- Published this work
- Found that BMP2 induced bone formation in the rat only occurs when implanted near skeletal bone. When implanted distal from the skeleton, no bone formation occurs. However if BMP2 is placed both close to the skeleton and distal, HO will progress in both locations.
- Shown that BMP2 appears to mobilize a set of progenitors from periosteum rather than peripheral nerves as in the mouse. However, the progenitors contributing to the establishment of the bone are strikingly similar between rat and mouse.
- Disclosed the phenotype and nature of the osteogenic progenitors
- Identified that the claudin 5^+ PDGFRα^+ osterix$^+$ cell appears to expand and migrate from the periosteum of skeletal bone towards the location of the BMP2 producing cells.
- Shown that transient brown adipocytes appear rapidly and co-localize with the migrating osteoprogenitors.
- Analyzed the rat nerves and found that neural progenitors similar to the mouse appear to respond by expanding but are unable to migrate from the nerve. These findings are similar to studies in the mouse where cromolyn is used to suppress mast cell degranulation.
- Shown that attempts to rescue HO in the rat by delivery of bone marrow mesenchymal stem cells resulted in no bone formation. However, isolation of the mouse nerve progenitors and delivery with the BMP2 producing cells resulted in restoring HO at the distal site.

CONCLUSION:

We have initiated experiments to isolate and characterize the potential M2 monocyte cells that we propose are involved in rapid remodeling of the skeletal bone matrix for integration to the newly formed bone fusion mass. In these experiments we have identified the initial cells and found that they possess several markers of the M2 lineage, which will be useful for fluorescence activated cell sorting. Once we have isolated these cells we will test their ability to resorb bone through a standard assay, and will also confirm that they behave similarly to M2 monocytes in their ability to respond to IL4 rather than proinflammatory cytokines such as LPS. These experiments are ongoing and we have not run into any problems that would prevent us from reaching our proposed goals. We have begun to establish optimal parameters for encapsulation of the MSCs-icasp9M in the PEG hydrogel microspheres that will lead to optimal bone formation. This included a number of preliminary *in vitro* experiments. We have developed a method for analyzing the microbeads through automated imaging software being developed at BCM to rapidly screen and quantify changes in the cells within the microspheres. We predict this work will be completed in the 6 months for publication.

We have also initiated studies with the degradable form of the hydrogel. Currently, we have produced a new batch of the polymer and are focused on looking at degradation *in vivo* through incorporation of the near infra-red dye into the polymer, and then measuring the signal overtime. We will do this in conjunction with the MSCs-icasp9M that has been transduced with AdRiFP, which can easily be separated from the near infrared reporter. Finally in these experiments we are also following bone formation through x-rays to reduce the amount of radiation exposure of the newly forming bone. However, this will allow us to focus on remodeling of the materials in the same animal. This work has been delayed by the problems associated with the rat model. We have been unable to get bone formation within the spine, and therefore have been held up on completing this work. Recently, we idenfitied key differences between the rat and mouse recruitment of osteoprogenitors, and now have a better understanding about how BMP2 may be inducing bone formation in this organism. Because of this, we are requesting to be allowed to continue the ongoing experiments in a mouse model, to develop this hydrogel and confirm the parameters for removal of the material with respect to the bone formation and termination of the cells through apopotsis. We can readily get back on track and complete all our deliverables if we are able to switch these material development studies back to the mouse, while we complete our work on understanding the biological mechanisms utilized by the rat. We propose to continue and complete the studies with the mouse hind limb system, and then advance into the mouse spine once we have the system working. Alternatively, if we complete the studies in the mouse hind limb, and have successfully been fusing the rat spine with minor modifications to our system, we will then move forward with the original rat model.

We will continue to characterize BMP2 induced bone formation in the rat model, and will hopefully be able to rescue the spine fusion through addition of either osteoprogenitors or MMP9. BMP2 induced targeted bone formation is very different in the mouse and rat as far as the source for recruiting stem cells. We noted that the rat appears to recruit osteoprogenitors similar to those in the mouse, but from the periosteum, and thus is forming bone only when near skeletal bone that has a functional periosteum. Further investigation of the adjacent peripheral nerves suggests that the same osteoprogenitors used in mouse are actually being expanded; however, they appear to be unable to leave the nerve, suggesting that perhaps the rat nerve structure, which has a much larger epineurial collagen matrix than mouse prevents activation of neuro-inflammatory pathways and epineurial remodeling (Salisbury *et al*, 2011, Salisbury *et al*, 2012). We have now shown that periosteum itself, or bone marrow derived mesenchymal stem cells do not rescue the bone formation in the presence of BMP2 if the target is distal from the skeletal periosteum. However, osteoprogenitors isolated from the mouse appear to rescue, and thus may support that this system is capable of delivering physiological levels of BMP2 for rapid bone formation at a targeted location, as long as adequate progenitors can mobilize. Studies are underway to complete and answer these questions. These studies will be completed and published in the next few months.

PUBLICATIONS, ABSTRACTS, AND PRESENTATIONS:

1. Lay Press: None
2. Peer-Reviewed Scientific Journals:

- Lu Y, Darne C, Tan I, Zhu B, Hall M, Lazard Z, Davis AR, Simpson S, Sevick-Muraca EM and **Olmsted-Davis EA**. Far-red fluorescence gene reporter tomography for determination of placement and viability of cell-based gene therapies. Opt Express. 2013 Oct 7;21(20):24129-38.
- Sonnet C, Olabisi R, Simpson C, Weh M, Peroni J, Gugala Z, Hipp JA, Gannon FH, Lindsey RW, Davis AR, West JL, and **Olmsted-Davis EA**. Injection of Osteoinductive Microspheres Leads to Rapid Healing of Critical Size Femoral Defects in Wild Type Rats. J. Orthop Res. 2013 Oct;31(10):1597-604.
- Lazard ZW, Salisbury EA, Gugala Z, Beal II E, Ubogu EH, **Olmsted-Davis EA**, and Davis AR. Neural Origins of Osteoblasts during Heterotopic Ossification. (In review, JBMR)
- Sonnet C, Davis EL, Lazard ZW, Nistal R, Salisbury EA, Beal II E, Gugala Z, Davis AR, **Olmsted-Davis EA**. The Absence of BMP2 Induced *De Novo* Bone Formation in a Rat. (In preparation)

3. Invited Articles:

- Reichel LM, Salisbury E, Moustoukas MJ, Davis AR, **Olmsted-Davis EA.** Molecular Mechanisms of Heterotopic Ossification. J Hand Surg Am. 2014 Mar;39(3):563-6.
- Davis EL, Davis AR and **Olmsted-Davis EA**. Different Strokes for Different Folks; A Comparison of Heterotopic Ossification in the Rat, Mouse, and Human. (In preparation)

4. Abstracts:

- **Olmsted-Davis EA**, Gugala Z, Salisbury EA, Lazard ZW, and Davis AR. Peripheral nerves are a significant reservoir of progenitor cells for bone formation in heterotopic ossification. 2014 Bones & Teeth Gordon Research Conference. Jan 26-31 Galveston, TX.
    - 1st place poster prize - $600
- **Olmsted-Davis EA**, Sonnet C, Salisbury EA, Lazard ZW, Beal II E, Forsberg J, Davis T, and Davis AR. Heterotopic Bone is derived in Large Part from Progenitors in Peripheral Nerves: Major Difficulties in Animal Models of BMP2 Testing. 2014 Musculoskeletal Biology & Bioengineering Gordon Research Conference. Aug 3-8, Andover, NH.
    - Invited Oral Presentation
- Lazard ZW, Salisbury EA, Gugala Z, Ubogu EH, **Olmsted-Davis EA**, and Davis AR. Neural Origin of Osteoblasts during Heterotopic Ossification. 2014 American Society for Bone and Mineral Research Annual Meeting. Sept 12-15, Houston, TX.
    - Selected as a plenary poster
- Sonnet C, Davis EL, Lazard ZW, Beal II E, Salisbury EA, Davis AR, and **Olmsted-Davis EA**. Animal Models Use Different Mechanisms for Bone Formation in Heterotopic Ossification: A Comparison of Mouse, Rat, and Human. 2014 American Society for Bone and Mineral Research Annual Meeting. 2014 American Society for Bone and Mineral Research Annual Meeting. Sept 12-15, Houston, TX.

INVENTIONS, PATENTS AND LICENSES: The microbeads were already submitted for patenting, in a previous year. We are currently in the process of submitted a disclosure for the claudin 5^+, PDGFRα^+, osterix$^+$ dlx 5^+ osteogenic progenitors.

Inventors: Alan R. Davis and Elizabeth A. Olmsted-Davis

REPORTABLE OUTCOMES: There are no additional new additional products; however, the osteinductive microspheres were licensed to RegenOST a new start up company started by BCM to develop the materials.

OTHER ACHIEVEMENTS: RegenOST has licensed the materials from BCM and has submitted a grant proposal to the NIH small business program to further develop the materials in a large animal (Macque) model.

REFERENCES: List all references pertinent to the report using a standard journal format (i.e. format used in *Science, Military Medicine*, etc.).

1. Lu Y, Darne C, Tan I, Zhu B, Hall M, Lazard Z, Davis AR, Simpson S, Sevick-Muraca EM and Olmsted-Davis EA. Far-red fluorescence gene reporter tomography for determination of placement and viability of cell-based gene therapies. Optics Express Opt Express. 2013 Oct7;21(20):24129-38 PMID 24104323
2. Salisbury EA, Rodenberg E, Sonnet C, Gannon FH, Shine D, Vadakkan T, Dickinson M, Olmsted-Davis EA, and Davis AR. Sensory Nerve Induced Inflammation Contributes to Heterotopic Ossification. J Cell Biochem. 2011 Oct;112 (10):2748-58. PMID:21678472
3. Salisbury EA, Lazard ZW, Ubogu EH, Davis AR and Olmsted-Davis EA. Transient Brown Adipocyte-Like Cells Derived from Peripheral Nerve Progenitors in Response to BMP2. Stem Cells Translational Medicine 2012 Dec;1(12):874-85 PMID:23283549
4. Sonnet C, Olabisi R, Simpson C, Weh M, Peroni J, Gugala Z, Hipp JA, Gannon FH, Lindsey RW, Davis AR, West JL, and Olmsted-Davis EA. Injection of Osteoinductive Microspheres Leads to Rapid Healing of Critical Size Femoral Defects in Wild Type Rats. J. Orthop Res. 2013 Oct;31(10):1597-604
5. Rodenberg E, Lazard ZW, Azhdarinia A, Hall M, Kwon S, Wilganowski N, Merched-Sauvage M, Salisbury EA, Davis AR, Sevick-Muraca EM, and Olmsted-Davis EA. Matrix Metalloproteinase-9 is a Diagnostic Marker of Heterotopic Ossification in a Murine Model. Tissue Eng Part A. 2011 Oct;17(19-20):2487-96. PMID:21599541

APPENDICES:

- Lazard ZW, Salisbury EA, Gugala Z, Beal II E, Ubogu EH, Olmsted-Davis EA, and Davis AR. Neural Origins of Osteoblasts during Heterotopic Ossification. (In review, JBMR)

Neural Origin of Osteoblasts during Heterotopic Ossification

ZaWaunyka W Lazard[1], Elizabeth A. Olmsted-Davis[1,2,3] , Elizabeth A Salisbury[1], Zbigniew Gugala[4], Eric Beal II[1], Eroboghene H. Ubogu[5], , and Alan R. Davis[1,2,3]

Center for Cell and Gene Therapy[1], Departments of Pediatrics, Hematology-Oncology[2] and Orthopedic Surgery[3]

Baylor College of Medicine

One Baylor Plaza

Houston, TX 77030

Department of Orthopedic Surgery and Rehabilitation[4]

University of Texas

School of Medicine

Galveston, TX 77555

Department of Neurology[5]

The University of Alabama at Birmingham

Birmingham, AL 35294

Bone morphogenetic protein type 2/heterotopic ossification/claudin 5/tight junctional molecules/blood-nerve barrier/blood-brain barrier/extravasation

Abstract

Introduction*:* Heterotopic ossification (HO) is the process of *de novo* bone formation at a non-skeletal site. Recently, we showed that the earliest steps in this process involve changes in sensory nerves. Here, we extend these studies by identifying unique osteogenic progenitors within the endoneurial compartment of nerves adjacent to the site of HO after delivery of sustained low-levels of bone morphogenetic protein type 2 (BMP2).

Materials and Methods: HO was induced by intramuscular injection of Ad5BMP2-transduced cells in mice. Osteoprogenitors were identified through immunohistochemistry then quantified and further characterized by fluorescence activated cell sorting (FACS) and immunocytochemistry.

Results: Induction of HO by low-dose BMP2 leads to the expression, within 24 h, of the osteoblast-specific transcription factors, *dlx5* and osterix in osteoprogenitors in the endoneurium of local peripheral nerves. This is then followed by their coordinate disappearance from the nerve and re-appearance in the circulation by 48 hours. During their exit from the nerve, these cells begin to express the tight junction molecule, claudin 5. These osterix^{+} claudin 5^{+} cells then disappear from circulation at approximately 3-4 days after delivery of BMP2 followed by coordinate reappearance at the site of bone formation. Concurrent with this reappearance, we observed significant elevated expression of factors involved in extravasation (CXCR4, E-selectin, and CD44) These endoneurial progenitors also expressed the neural markers PDGFRα, the low-affinity nerve growth factor receptor (p75(NTR) and the neural crest stem cell marker musashi-1 as well as the endothelial marker Tie-2. They were distinct from the perineurial-like progenitors we previously described that form the transient brown adipocytes (1).

Conclusions: We conclude that these endoneurial progenitors are osteogenic precursors that are utilized for heterotopic ossification.

Introduction

Osteoblasts have long been thought to be uniquely derived from the bone marrow mesenchymal stem cells (2). However, several alternate mechanisms have recently been noted including the description of circulating osteoprogenitors that are osteocalcin$^+$ and osteopontin$^+$ (3-5) as well as the presence of osteoprogenitors that take on the characteristics of endothelial cells before being incorporated as osteoblasts in heterotopic ossification (6). Recent studies suggest the presence of a local stem/progenitor cell that could become a fully differentiated osteoblast in models of heterotopic ossification (HO) (6,7) (8). Initial reports of such a localized osteoprogenitor suggested that it may be a muscle satellite (9) or smooth muscle cell (10), which in the presence of BMP2, expanded and underwent osseous differentiation. However, Lounev *et al*, through lineage tracing for the hematopoietic-endothelial marker Tie-2, demonstrated the presence of reporter in the immature fibroproliferative cells as well as the osteogenic cells within HO, suggesting that the cells were endothelial in origin (7). They also found that the smooth muscle marker, smooth muscle myosin heavy chain (SMMHC) and skeletal muscle marker (MyoD) were observed in less than 5% of the cells. Opposing this theory, Wosczyna *et al* using a similar lineage tracing system, suggested that the Tie-2$^+$ PDGFRα$^+$ Sca-1$^+$ myoD$^-$ progenitor is distinct from the vascular endothelium and resides in the interstitial region of skeletal muscle (9). They demonstrated that the native endothelial cells did not participate in HO, nor did exogenously delivered endothelial cells previously exposed to BMP2. Setting them apart from previously described muscle stem cell populations, these progenitors were negative for myoD, pericyte markers, did not share a basal lamina with the adjacent endothelium, and appeared to be a totally distinct cell population.

In support of these findings, studies of human heterotopic ossification in the military population suggest the presence of a mesenchymal stem cell expressing PDGFRα (11). Furthermore, HO observed in military patients often involves or encompasses the peripheral nerves, termed neurovascular entrapment, making it difficult to surgically remove (12). However, all studies agree that the progenitor possesses the neural/glial cell-specific receptor PDGFRα (13,14) (15).

We previously demonstrated a link between peripheral nerves and HO in a murine model, which relies on sustained delivery of BMP2 through injection of AdBMP2- transduced cells into muscle (8). Although these cells are rapidly cleared within four days, they express low levels of BMP2, at a maximum 50 ng total, and launch a series of events that leads to mineralized bone within 7 days (16) (17) (18) (19). Salisbury *et al* (8)

identified the immediate expression of the pain mediators, substance P and GCRP, upon delivery of the BMP2, which leads to neural inflammation with resultant degranulation of local mast cells and remodeling of the epineurium. Removal of the epineurium was correlated with migration of progenitors that reside in the perineurium that undergo brown adipogenesis (1), presumably for the purpose of patterning the new bone (20). Blocking this process through delivery of inhibitors of mast cell degranulation (8) or binding of pain mediators to their receptor (21) resulted in a significant decrease in HO. Blocking nerve remodeling led to the accumulation within the endoneurium of nanog^{+} Klf-4^{+} osterix^{+} progenitors (22).

The endoneurium contains the axons and their supporting glial cells, called Schwann cells, embedded in loose collagen fibrils within unique fascicles surrounded by multiple layers of perineurial cells (23,24). The endoneurium possesses a tight junction forming microvascular barrier similar to that found in the brain. This barrier is critical in control of the endoneurial microenvironment needed to maintain normal axonal signal transduction and is known as the blood-nerve barrier (BNB) (25). An important protein, claudin 5, has been shown to be an essential component of restrictive microvascular barriers. This protein is expressed at sites of cell-to-cell contact on human endoneurial endothelial cells *in vitro* (26) (27). Mice lacking expression of claudin 5 lack a functional blood-brain barrier (BBB) and die immediately after birth (28).

Here we extend these studies to further characterize the osterix^{+} cells residing in nerve to determine if they are derived from stem and/or progenitor cells within the endoneurium, or from pre-existing differentiated cells, such as endothelial or Schwann cells, which also reside in this region. These studies suggest that a neural progenitor resides within the endoneurial compartment of local peripheral nerves that starts to express osterix and rapidly migrates through the tight junction of the nerve into the circulation allowing it to home to the site of newly forming bone. Thus, our data supports both the presence of localized progenitors as well as a circulating cell and provides a novel connection between heterotopic ossification and sensory nerves.

Materials and Methods

Cell Culture: A murine fibroblast cell line was obtained from the American Type Culture Collection (Manassas, VA) and propagated in α-minimum essential medium (α-MEM). This cell type is not capable of inducing bone formation before transduction. The cell line was supplemented with 10% fetal bovine serum (HyClone, Logan,, UT), penicillin (100 units/mL), streptomycin (100µg/mL) and amphotericin B (25 µg/mL) (Invitrogen Life Technologies, Gaithersburg, MD). The cell line was grown at 37°C and 5% CO2 in humidified air.

Heterotopic Bone Assay: Replication defective E1- to E3- deleted human adenovirus type 5 fiber protein (Ad5) was constructed to contain cDNAs for BMP2 in the E1 region of the virus (16) or did not contain any transgene in this region, Ad Empty. The resultant purified viruses, AdBMP2 and Ad Empty cassette, had viral particle(VP)-to-plaque-forming unit (PFU) ratios of 1:77 and 1:111, respectively, and all viruses were confirmed to be negative for replication competent adenovirus (16). Cells were transduced as previously described with AdBMP2 or Ad Empty cassette at a viral concentration of 5,000VP/cell with 1.2% Gene Jammer (18) (19). MC3T3-E1 cells lack the receptor for Ad5, the coxsackievirus-adenovirus receptor (CAR) and therefore GeneJammer is used to efficiently transduce the cells. Adenovirus was allowed to incubate overnight at 37°C, humidified atmosphere and 5% CO2. The transduced cells were resuspended at a concentration of $5x10^6$ cells per 100µL of PBS and delivered by intramuscular injection into the hind limb quadriceps muscle of C57BL/6 (Jackson Laboratory Repository, Bar Harbor, ME).

Immunohistological and immunocytochemcial analysis: For paraffin sections the entire hind limb including the skeletal bone was harvested, the skin was removed, then the tissue was decalcified and paraffin embedded. For frozen sections the soft tissue encompassing the site of the new bone formation were isolated from the rear hind limbs and flash frozen. Serial sections (3-4 µm) were prepared with approximately 50 sections per tissue specimen. Hematoxylin and eosin staining was performed on every tenth slide in order to locate the region containing our delivery cells or the newly forming endochondral bone. Serial unstained slides were used for immunohistochemical staining with either single or double antibody labeling. Primary antibodies were added to slides at a dilution of 1:100 to 1:200 with an overnight incubation, washed and incubated with respective secondary antibodies of either Alexa Fluor 488, 594 or 647 (Invitrogen Life Technologies) at a 1:500 dilution. Primary antibodies were used as follows: Claudin 5 (Novus Biological), CD31 (BD Pharmingen),

Neurofilament (NF) (Sigma-Aldrich), osterix (OSX) (R & D systems), Tie 2 (Chemicon), *dlx 5* (Santa Cruz), [CD44, E-selectin (CD62), myelin protein 0 (p0), Musashi 1 (NRP-1), nerve growth factor receptor (NGF, p75)] [Abcam]. Primary and secondary antibodies were diluted in 2% bovine serum albumin or the mouse on mouse, M.O.M. kit, (Vector Laboratories) was used according to manufacturer protocol for mouse antibodies. Tissues were counterstained and covered with Vectashield mounting medium containing DAPI (Vector Laboratories).

Cytospin slide preparations of FACS isolated cells were produced by centrifugation of approximately 40,000 cells at 500 rpm, using a Cytopro 7620 cytocentrifuge (Wescor), for 5 minutes. The slides were subsequently immunostained following similar methods as above. Briefly, cells were fixed with 4% paraformaldehyde, PBS washed, treated with 0.3% Triton X-100 in 0.3% Tris-buffered saline, blocked with 2% BSA, and incubated in primary antibody overnight. After PBS washing, samples were incubated in the appropriate secondary antibody and counterstained with DAPI. Stained cells were examined by confocal microscopy (LSM 510 META, Zeiss, Inc.).

Flow Cytometry and Fluorescence Activated Cell Sorting (FACS): Cells isolated from the hind limb soft tissues after removal of the skeletal bone, and skin. Briefly, soft tissues were isolated from 3 mice (both legs pooled as one replicate) minced with scissors, and then subject to 0.2% collagenase type II digestion at 37 C for 45 minutes. The digestion was stopped by adding an equal volume of DMEM containing 10% FBS and cells collected by centrifugation at 400 X g for 5 minutes. Debris was removed by filtering with a 70 micron filter. For isolation of cells from peripheral blood, whole blood was layered onto Ficoll-Paque^{TM} Plus (GE Healthcare) and spun according to manufacturer's instructions. The mononuclear cell band was removed, washed with PBS and then immunostained as follows. The cells were next incubated with Claudin 5 antibody (Novus Biological,1:200 dilution) and/or PDGFRα (Santa Cruz) for 45 minutes on ice. Cells were washed with 1X phosphate buffered saline (PBS) and then incubated with anti-goat Alexa Fluor 488 (Invitrogen, 1:500 dilution) for 30 minutes on ice. Cells were again washed with 1X PBS and stained cells were analyzed on a FACSAria II (BD, Becton Dickson) flow cytometer and BD FACSDiva Software. For cell sorting, labeled cells were separated based on their fluorescence intensity and the Claudin 5 negative and positive population were collected with >95% purity. The percentage of positive cells from each experiment was averaged, the standard

error of the mean calculated, and statistical significance was determined by ANOVA with Bonferroni-Holm post-hoc correction for multiple comparisons.

Q-RT-PCR (Real Time PCR) From the harvested muscle tissue surrounding the injection site of either control or BMP2 transduced cells, total RNA was collected using a Trizol reagent (Life Technologies, Carlsbad, CA). RNA integrity was confirmed by agarose gel electrophoresis. cDNA was synthesized from RNA using the RT2 first strand kit (SA Biosciences Inc., Frederick, MD). The cDNA from each sample was analyzed separately, the results were averaged and standard error of the mean calculated. The cDNA from muscles with control or BMP2 transduced cells were subjected to qRT-PCR analysis in parallel using a 7900HT PRISM Real-Time PCR machine (Applied Biosystems, Carlsbad, CA). The C_t values were normalized to both internal 18S ribosomal RNA used in multiplexing and to each other to remove changes in gene expression common to both the control and BMP-2 tissues by using the method of $\Delta\Delta$ C_t along with SYBR Green probes and qPCR primers (SABiosciences, Frederick, MD). The analyses were conducted in triplicate for 8 biological samples at each time point and were reported as the average and standard deviation of the fraction of RNA that was attributed to target cDNA. Significance was determined by ANOVA with Bonferroni-Holm post-hoc correction for multiple comparisons.

Results

BMP2 induces the appearance of osterix in p75$^+$ cells in the endoneurium of peripheral nerves: Previous studies (8) suggested that cells present in the endoneurial compartment of peripheral nerves express the osteogenic factor osterix after delivery of AdBMP2-transduced cells.. Therefore tissues were isolated and immunostained on days 1, 2, 4, and 7 after induction of HO through delivery of AdBMP2-transduced cells. Surprisingly, there was significant osterix expression on cells in the endoneurium at 24 h, but this rapidly disappeared within 24 hours as seen on tissues isolated 2 days after induction of HO (Figure 1A). Note in Figure 1A two different primary antibodies represented by two different secondary antibodies were used to confirm this phenomenon and patterns of osterix expression appeared to be similar, independent of the antibody. To confirm the nerve structure, tissues were also immunostained with neurofilament H chain (NF). Two cell types are common within the endoneurial compartment of peripheral nerves, specialized vascular endothelial cells and Schwann cells necessary for myelination of axons. Claudin 5 has previously been shown to be a marker for the specialized endoneurial endothelial cells (26,27). Therefore, tissues were co-stained for osterix and claudin 5 (Figure 1). As expected, claudin 5 appeared to be associated with vessels and the expression pattern matching CD31$^+$ vasculature is shown on a serial section (Figure 1A). Interestingly, the majority of the claudin 5$^+$ cells did not appear to co-align with osterix. However by the second day after induction, some of the vessels within the endoneurium express both claudin 5 and CD31, although it is not clear whether osteoprogenitors in these vessels co-express these proteins. Examination of tissues isolated 4 and 7 days after BMP2 induction (Figure 1B) shows co-expression of osterix and claudin 5 in many cells throughout the muscle. Additionally, substantial vessel networks, as assessed by CD31 staining (red, Figure 1B), were observed in the region where the claudin 5$^+$ osterix$^+$ cells were localized, and these regions were found by day 7 to be associated with bone matrix (Figure 1B, yellow arrows). The data suggests that osteoprogenitors outside the nerve express claudin 5, however the osterix$^+$ cells in the endoneurium 24 hours after delivery of BMP2 do not appear to express claudin 5.

We next immunostained cells for the presence of two Schwann cell markers, low-affinity nerve growth factor receptor (p75 (NTR) and myelin protein zero (MPZ) (Figure 1C). It has been previously demonstrated that Schwann cells express elevated levels of p75 (NTR) during peripheral nerve regeneration and myelination

(29). However, it has also been shown that neural crest stem cells express p75 (NTR) (30). To distinguish Schwann cells from neural progenitors, tissues isolated at 2 days and 6 days after induction of HO were co-immunostained with osterix and either p75 (NTR) or myelin protein zero (MPZ). The results show the co-expression of osterix and p75 within the endoneurium (Figure 1C). MPZ^+ cells were also observed in this region of the nerve; however these cells did not express osterix (Figure 1C). The results suggest that the osterix $^+$ cell within in the endoneurium is either a Schwann cell that is not myelinating or a neural progenitor that resides in the endoneurium of adult nerves as previously described by Morrison et al , 1999 (30).

Claudin 5$^+$ osteoprogenitors enter the general circulation shortly after BMP2 induction: Osterix expression was present on the endoneurial cells for only 24 hours after which time we did not observe expression in the nerve (Figure 1A). This suggests that either expression is down regulated or that these cells immediately exit the nerve. One of the only ways for cells to exit the endoneurium of the nerve is through the highly regulated blood-nerve barrier formed by tight and adheren junctions between endoneurial endothelial cells lining the endoneurial vessels. Since claudin 5 is not only an important tight junction protein, but also has been found in blood after barrier disruption (31), mononuclear cells from blood were isolated and tested for the presence of claudin 5^+ cells at various times after BMP2 induction. The results show that approximately 1 percent of the cells were positive for claudin 5 one day after induction of bone formation, and this was not significantly different from the control. Interestingly, the percentage of claudin 5^+ cells increased dramatically two days after the induction, with approximately 4.5% of the cells now positive for this marker. However, the increase in cells expressing claudin 5 in blood was short-lived and levels returned to background four days after BMP2 induction (Figure 2A).

To confirm that these circulating claudin 5^+ cells were expressing osterix, both positive and negative populations were isolated by FACS followed by cytospin and immunostaining for osterix. All of the osterix expression was found to be expressed in the claudin 5^+ cells (Figure 2B). The data collectively suggests that cells in the endoneurium that express osterix rapidly exit the nerve through vascular tight junctions that are

regulated in part by claudin 5. Upon entering the endoneurial vessels it appears that osteoprogenitors begin to express claudin 5, although the reason for such expression is unclear.

Osteoprogenitors extravasate across the vessel wall when they reach the area of bone formation: To determine if the process of extravasation (32) is involved in the migration of the claudin 5^+ osterix$^+$ cells through the vessel wall and to the site of bone formation, RNA was isolated from muscle at daily intervals for seven days after BMP2 induction and known extravasation factors (CXCR4, CD44, SDF, and P and E-selectin) were quantified through qRT-PCR (Figure 3A). The results show a significant increase in CXCR4, CD44 and E-selectin RNAs starting 4 days after induction of HO that was maintained for the remainder of bone formation (Figure 3A), whereas SDF and P-Selectin did not show a significant change (data not shown). As confirmation, claudin 5^+ and $^-$ cells were isolated from the tissues, spun onto slides that were then immunostained for a factor present on the endothelial cells (E-selectin) as well as factors present on the extravasating cell (CD44 and CXCR4) As expected, the claudin 5^+ population expressed CD44 and CXCR4 whereas the negative population expressed E-selectin (Figure 3B), suggesting that extravasation through the vessel wall is responsible for the engraftment of the cells at the site of bone formation.

Claudin 5^+ cells express osteogenic markers after BMP2 induction: Claudin 5^+ and $^-$ populations of cells were isolated from the tissues surrounding the site of new bone formation four days after BMP2 induction (Figure 4). Cells were immunostained for the osteogenic factors osterix and *dlx 5*. Surprisingly, the majority (90%) of the claudin 5-positive population also stained positively for osterix (Figure 4, panels A-C). Although there were numerous cells in the claudin 5^-negative population, as determined by DAPI staining (panel F), there were virtually no cells staining positively for osterix (Figure 4 panel E). We next performed immunostaining to detect the expression of dlx5 on the claudin 5^+ and $^-$ cell populations. Dlx5 is an osteogenic factor that is expressed during development in the perichondrial region of both the embryonic axial and appendicular skeleton (33) and is thought to be upstream of osterix. It is activated by BMP2 and upregulates both osterix (34) and osteocalcin (30) expression during osteogenesis. Dlx 5 was expressed only in the

claudin 5^+ cell population, although some of the cells were not positive for this factor (Figure 4, panels G-I) the claudin 5^- population was completely negative for dlx5 expression (Figure 4, panel K).

Claudin 5^+ cells express factors associated with nerve stem/progenitor cells: Claudin 5^+ cells were further characterized for the expression of two additional nerve stem/progenitor cell markers, PDGFRα and musashi. Both PDGFRα, a factor associated with perivascular astrocytes (15) and shown to be involved in glial-endothelial cell interactions and critical for maintenance of the blood-brain barrier (15), and musashi, which is an RNA binding protein that is highly specific for neural stem cells (33) and is not expressed in fully differentiated cells (34) (35), were assessed on the claudin 5^+ cells. FACS analysis showed that PDGFRα was expressed on these cells (Figure 5A). Analysis of the cells showed the absence of a claudin 5^+ PDGFRα$^-$ population although we did observe a small PDGFRα$^+$ claudin 5^- population (Figure 5A) that may represent Schwann cells, which previously have been shown to be positive for this receptor (36).

Again claudin 5^+ and $^-$ populations isolated from tissues two days after delivery of the AdBMP2-transduced cells were isolated and immunostained for musashi. Almost all the cells in the claudin 5^+ population were also musashi$^+$ (Figure 5B, panels G-I). Positive immunostaining for musashi was not observed in the claudin 5^- population although there were an equal number of cells on the slides (Figure 5B, panels J-L). Overall the data suggests that these osteoprogenitor cells, in addition to the upregulation of osteogenic factors, also express neural crest markers, which may be remnants of their neural origin.

Claudin 5^+ cells express the endothelial marker Tie-2: Since others have reported the presence of PDGFRα on the surface of an osteoprogenitor expressing Tie 2, the claudin 5^+ and $^-$ populations were immunostained for Tie-2 (Figure 6A). Almost all of the claudin 5^+ cells were found to express Tie-2, but there appeared to be a wide variation in its expression level (Figure 6A). Additionally, we noted that in some cases Tie 2 had a surprisingly asymmetric localization on cells (Figure 6B), which may indicate a migrating, rather than matrix bound, cell as described by Saharinen *et al* (37). The data collectively suggest that these osteoprogenitors express not only osteogenic transcription factors (osterix and dlx 5), but also markers of early neural (mushasi and PDGFα), and vascular (Tie-2) progenitors. Hence the progenitors, although bound for a

potentially unique destination (bone), are expressing a variety of markers that may allow them to be recruited for a variety of fates.

Discussion

The results show the presence of osterix$^+$ cells in the endoneurium of peripheral nerves immediately after HO induction through delivery of AdBMP2 transduced cells. These cells then disappear at the same time as the appearance of osterix$^+$ claudin 5$^+$ cells in the circulation. Within four days after induction of HO they disappear from the blood stream simultaneously with an increase in expression of factors involved in cell extravasation and the appearance of the osterix$^+$ claudin 5$^+$ cells in muscle at the site of heterotopic ossification. The data suggests that these osteoprogenitors exit the nerve through the blood-nerve barrier, enter the circulation, and home to the site of HO.

The reason for expression of claudin 5 by these osteoprogenitors is not clear. It has been shown that cells expressing claudin 5 have not only increased adherence, but also increased motility (38) consistent with the ability of these osteoprogenitors to circulate. Interestingly, endothelial progenitors have previously been shown to leave the vessel wall and circulate (39) suggesting that the osterix$^+$ claudin 5$^+$ p75$^+$ cells may function similarly to these endothelial progenitors.

These osterix$^+$ claudin 5$^+$ p75$^+$ cells then appear to home to the site of bone formation. We previously showed the rapid expansion of new vessels after delivery of the AdBMP2- transduced cells (40) and in the current study an extensive vascular plexus can be seen surrounding the claudin 5$^+$ osterix$^+$ cells. Further, at this same time, extravasation factors (CXCR4, CD44, and E-selectin) were significantly elevated in these tissues consistent with the appearance, through the circulation, of the cells at this site. It has been previously shown that CD44 is a key mediator of the transendothelial migration of many cell types and mediates the binding of CD44 to hyaluronic acid on the endothelial cell (41) (32,42). Further, invasion of calcified cartilage by vessels is a key event in endochondral bone formation (43). Therefore, CD44 which is expressed on the surface of the osteoprogenitor likely binds to the E-selectin on the surface of the endothelial cells. This is the first step of extravasation. Additionally the cells appear to express CXCR4, which is also significantly elevated in the tissues at this time; CXCR4 has been shown to bind SDF 1 on endothelial cells, as the second step in extravasation, which allows for tighter binding, and eventually migration through pores between the endothelial

cells (44). The change in SDF 1 RNA within the tissues did not change significantly during HO; however, it was present in the tissues (data not shown). Additionally the new vessels that are rapidly forming at this site are tiny with the significant branches, suggesting lower flow, necessary for depositing cells. Finally new vessels or venules must undergo remodeling to organize the structure and support greater blood flow without leaking (45). Thus it is highly likely at this stage for cells to traverse the vessel wall more easily than in mature vessels.

Phenotypic characterization of these cells shows expression of Tie-2, a marker of endothelial cells. The presence of endothelial markers on osteoprogenitors has also recently been described by others (46) (6). Additionally these cells express musashi and p75 phenotypic markers of neural crest stem cells (33) (30,34,35). In addition to these neural crest markers, the cells also express PDGFRα, a factor involved in glial-endothelial cell interactions and critical for maintenance of the blood-brain barrier, suggesting that endothelial-neural cell interaction may play a key role in transition of these progenitors from a neural to mesodermal fate.

It is possible that BMP2 induction of bone formation in the adult is, at least in part, a re-capitulation of embryonic bone formation. The formation of craniofacial bone and cartilage in the embryo begins with neural crest stem cell migration from the neural tube (47). One of the key factors that indicate the start of osteogenesis in these cells is the expression of dlx5 and osterix, similar to the early osteogenic factors on the osterix^{+} claudin 5^{+} p75^{+}progenitors.. The synthesis of osteoblasts from neural crest stem cells uses a combination of Wnt and BMP signaling. Although Wnt 1 is the major inducer of neural crest (48), when it is unopposed Wnt 1 signaling leads to the production of sensory nerves from neural stem cells (49). However, when opposed by BMP2, Wnt 1 signaling in neural crest stem cells leads to other cell types including osteoprogenitors (50). Thus the biogenesis of osteoprogenitors in the adult may ultimately originate from neural stem cells housed in the endoneurium. It is conceivable that these cells may have been deposited within the endoneurium during neural crest migration and formation of sensory nerves. Perhaps neural crest stem cells are deposited in all neural crest tissues, since several reports suggest a Wnt1+ neural crest stem cell in the jaw. Alternatively, these cells may simply persist in the endoneurium because it is an immune privileged location. Therefore, they were never exposed to and cleared by the adult immune system. Such a mechanism would also allow tissue regeneration using a recapitulation of an embryonic process.

The current study also underscores the importance of barriers or interfaces between blood and nerves in heterotopic ossification. Two molecules that show dramatic increase upon BMP2 induction of heterotopic ossification, claudin 5 and PDGFRα are either a key component or regulator, respectively, of these barriers. Recently it has become very obvious that there is a relationship between traumatic brain injury and HO (51). One possible reason that HO is associated with traumatic brain injury, which causes a breakdown in the blood-brain barrier (51,52) could be that changes in this barrier, leads to the exit of these neural progenitors that can engraft and become osteoblasts, particularly at sites where BMP2 may be present such as those that have also sustained a fracture.

The data collectively suggests that neural progenitors within the endoneurium of peripheral nerves can undergo osteogenic differentiation, and migrate from the nerve, through the circulation to the site of new bone formation. Many recent studies suggest that osteoprogenitors are local progenitors, either recruited from vasculature or from interstitial spaces between muscle fibers (6) (7). Our data actually supports not only a circulating progenitor, but also a local progenitor, because the cells engraft several days prior to the appearance of cartilage or bone. Therefore these fibroblast-like cells deposited between the muscle fibers, would appear to be local cells. Further, if this is a recapitulation of neural crest formation of the bones and cartilage of the head, then presumably this is not endochondral bone formation but rather two independent processes. Thus, it may not be surprising that these osteogenic cells appear in a location distinct from the cartilage and arrive prior to its formation. In conclusion, these studies are the first to demonstrate the presence of a progenitor within peripheral nerves that responds to BMP2 by undergoing both osteogenic differentiation and homing to the location of bone formation.

References

1. Salisbury EA, Lazard ZW, Ubogu EE, Davis AR, Olmsted-Davis EA 2012 Transient brown adipocyte-like cells derive from peripheral nerve progenitors in response to bone morphogenetic protein 2. Stem Cells Transl Med **1**(12)**:**874-85.
2. Pittenger MF, Mackay AM, Beck SC, Jaiswal RK, Douglas R, Mosca JD, Moorman MA, Simonetti DW, Craig S, Marshak DR 1999 Multilineage potential of adult human mesenchymal stem cells. Science **284**(5411)**:**143-7.

3. Suda RK, Billings PC, Egan KP, Kim JH, McCarrick-Walmsley R, Glaser DL, Porter DL, Shore EM, Pignolo RJ 2009 Circulating osteogenic precursor cells in heterotopic bone formation. Stem Cells **27**(9)**:**2209-19.
4. Kumagai K, Vasanji A, Drazba JA, Butler RS, Muschler GF 2008 Circulating cells with osteogenic potential are physiologically mobilized into the fracture healing site in the parabiotic mice model. J Orthop Res **26**(2)**:**165-75.
5. Otsuru S, Tamai K, Yamazaki T, Yoshikawa H, Kaneda Y 2008 Circulating bone marrow-derived osteoblast progenitor cells are recruited to the bone-forming site by the CXCR4/stromal cell-derived factor-1 pathway. Stem Cells **26**(1)**:**223-34.
6. Medici D, Shore EM, Lounev VY, Kaplan FS, Kalluri R, Olsen BR 2010 Conversion of vascular endothelial cells into multipotent stem-like cells. Nat Med **16**(12)**:**1400-6.
7. Lounev VY, Ramachandran R, Wosczyna MN, Yamamoto M, Maidment AD, Shore EM, Glaser DL, Goldhamer DJ, Kaplan FS 2009 Identification of progenitor cells that contribute to heterotopic skeletogenesis. J Bone Joint Surg Am **91**(3)**:**652-63.
8. Salisbury E, Rodenberg E, Sonnet C, Hipp J, Gannon FH, Vadakkan TJ, Dickinson ME, Olmsted-Davis EA, Davis AR 2011 Sensory nerve induced inflammation contributes to heterotopic ossification. J Cell Biochem **112**(10)**:**2748-58.
9. Wosczyna MN, Biswas AA, Cogswell CA, Goldhamer DJ 2012 Multipotent progenitors resident in the skeletal muscle interstitium exhibit robust BMP-dependent osteogenic activity and mediate heterotopic ossification. J Bone Miner Res **27**(5)**:**1004-17.
10. Cairns DM, Liu R, Sen M, Canner JP, Schindeler A, Little DG, Zeng L 2012 Interplay of Nkx3.2, Sox9 and Pax3 regulates chondrogenic differentiation of muscle progenitor cells. PLoS One **7**(7)**:**e39642.
11. Jackson WM, Aragon AB, Bulken-Hoover JD, Nesti LJ, Tuan RS 2009 Putative heterotopic ossification progenitor cells derived from traumatized muscle. J Orthop Res **27**(12)**:**1645-51.
12. Polfer EM, Forsberg JA, Fleming ME, Potter BK 2013 Neurovascular entrapment due to combat-related heterotopic ossification in the lower extremity. J Bone Joint Surg Am **95**(24)**:**e195(1-6).
13. Pringle N, Collarini EJ, Mosley MJ, Heldin CH, Westermark B, Richardson WD 1989 PDGF A chain homodimers drive proliferation of bipotential (O-2A) glial progenitor cells in the developing rat optic nerve. EMBO J **8**(4)**:**1049-56.
14. Richardson WD, Pringle N, Mosley MJ, Westermark B, Dubois-Dalcq M 1988 A role for platelet-derived growth factor in normal gliogenesis in the central nervous system. Cell **53**(2)**:**309-19.
15. Su EJ, Fredriksson L, Geyer M, Folestad E, Cale J, Andrae J, Gao Y, Pietras K, Mann K, Yepes M, Strickland DK, Betsholtz C, Eriksson U, Lawrence DA 2008 Activation of PDGF-CC by tissue plasminogen activator impairs blood-brain barrier integrity during ischemic stroke. Nat Med **14**(7)**:**731-7.
16. Olmsted-Davis EA, Gugala Z, Gannon FH, Yotnda P, McAlhany RE, Lindsey RW, Davis AR 2002 Use of a chimeric adenovirus vector enhances BMP2 production and bone formation. Hum Gene Ther **13**(11)**:**1337-47.
17. Gugala Z, Olmsted-Davis EA, Gannon FH, Lindsey RW, Davis AR 2003 Osteoinduction by ex vivo adenovirus-mediated BMP2 delivery is independent of cell type. Gene Ther **10**(16)**:**1289-96.
18. Fouletier-Dilling CM, Bosch P, Davis AR, Shafer JA, Stice SL, Gugala Z, Gannon FH, Olmsted-Davis EA 2005 Novel compound enables high-level adenovirus transduction in the absence of an adenovirus-specific receptor. Hum Gene Ther **16**(11)**:**1287-97.
19. Fouletier-Dilling CM, Gannon FH, Olmsted-Davis EA, Lazard Z, Heggeness MH, Shafer JA, Hipp JA, Davis AR 2007 Efficient and rapid osteoinduction in an immune-competent host. Hum Gene Ther **18**(8)**:**733-45.
20. Olmsted-Davis E, Gannon FH, Ozen M, Ittmann MM, Gugala Z, Hipp JA, Moran KM, Fouletier-Dilling CM, Schumara-Martin S, Lindsey RW, Heggeness MH, Brenner MK, Davis AR 2007 Hypoxic adipocytes pattern early heterotopic bone formation. Am J Pathol **170**(2)**:**620-32.
21. Kan L, Lounev VY, Pignolo RJ, Duan L, Liu Y, Stock SR, McGuire TL, Lu B, Gerard NP, Shore EM, Kaplan FS, Kessler JA 2011 Substance P signaling mediates BMP-dependent heterotopic ossification. J Cell Biochem **112**(10)**:**2759-72.
22. Nakashima K, Zhou X, Kunkel G, Zhang Z, Deng JM, Behringer RR, de Crombrugghe B 2002 The novel zinc finger-containing transcription factor osterix is required for osteoblast differentiation and bone formation. Cell **108**(1)**:**17-29.

23. Mizisin AP, Weerasuriya A 2011 Homeostatic regulation of the endoneurial microenvironment during development, aging and in response to trauma, disease and toxic insult. Acta Neuropathol **121**(3)**:**291-312.
24. Weerasuriya A, Mizisin AP 2011 The blood-nerve barrier: structure and functional significance. Methods Mol Biol **686:**149-73.
25. Yosef N, Ubogu EE 2013 An immortalized human blood-nerve barrier endothelial cell line for in vitro permeability studies. Cell Mol Neurobiol **33**(2)**:**175-86.
26. Yosef N, Xia RH, Ubogu EE 2010 Development and characterization of a novel human in vitro blood-nerve barrier model using primary endoneurial endothelial cells. J Neuropathol Exp Neurol **69**(1)**:**82-97.
27. Ubogu EE 2013 The molecular and biophysical characterization of the human blood-nerve barrier: current concepts. J Vasc Res **50**(4)**:**289-303.
28. Nitta T, Hata M, Gotoh S, Seo Y, Sasaki H, Hashimoto N, Furuse M, Tsukita S 2003 Size-selective loosening of the blood-brain barrier in claudin-5-deficient mice. J Cell Biol **161**(3)**:**653-60.
29. Cosgaya JM, Chan JR, Shooter EM 2002 The neurotrophin receptor p75NTR as a positive modulator of myelination. Science **298**(5596)**:**1245-8.
30. Morrison SJ, White PM, Zock C, Anderson DJ 1999 Prospective identification, isolation by flow cytometry, and in vivo self-renewal of multipotent mammalian neural crest stem cells. Cell **96**(5)**:**737-49.
31. Kazmierski R, Michalak S, Wencel-Warot A, Nowinski WL 2012 Serum tight-junction proteins predict hemorrhagic transformation in ischemic stroke patients. Neurology **79**(16)**:**1677-85.
32. Rampon C, Weiss N, Deboux C, Chaverot N, Miller F, Buchet D, Tricoire-Leignel H, Cazaubon S, Baron-Van Evercooren A, Couraud PO 2008 Molecular mechanism of systemic delivery of neural precursor cells to the brain: assembly of brain endothelial apical cups and control of transmigration by CD44. Stem Cells **26**(7)**:**1673-82.
33. Nakamura M, Okano H, Blendy JA, Montell C 1994 Musashi, a neural RNA-binding protein required for Drosophila adult external sensory organ development. Neuron **13**(1)**:**67-81.
34. Okano H, Kawahara H, Toriya M, Nakao K, Shibata S, Imai T 2005 Function of RNA-binding protein Musashi-1 in stem cells. Exp Cell Res **306**(2)**:**349-56.
35. Battelli C, Nikopoulos GN, Mitchell JG, Verdi JM 2006 The RNA-binding protein Musashi-1 regulates neural development through the translational repression of p21WAF-1. Mol Cell Neurosci **31**(1)**:**85-96.
36. Eccleston PA, Funa K, Heldin CH 1993 Expression of platelet-derived growth factor (PDGF) and PDGF alpha- and beta-receptors in the peripheral nervous system: an analysis of sciatic nerve and dorsal root ganglia. Dev Biol **155**(2)**:**459-70.
37. Saharinen P, Eklund L, Miettinen J, Wirkkala R, Anisimov A, Winderlich M, Nottebaum A, Vestweber D, Deutsch U, Koh GY, Olsen BR, Alitalo K 2008 Angiopoietins assemble distinct Tie2 signalling complexes in endothelial cell-cell and cell-matrix contacts. Nat Cell Biol **10**(5)**:**527-37.
38. Escudero-Esparza A, Jiang WG, Martin TA 2012 Claudin-5 is involved in breast cancer cell motility through the N-WASP and ROCK signalling pathways. J Exp Clin Cancer Res **31:**43.
39. Asahara T, Murohara T, Sullivan A, Silver M, van der Zee R, Li T, Witzenbichler B, Schatteman G, Isner JM 1997 Isolation of putative progenitor endothelial cells for angiogenesis. Science **275**(5302)**:**964-7.
40. Dilling CF, Wada AM, Lazard ZW, Salisbury EA, Gannon FH, Vadakkan TJ, Gao L, Hirschi K, Dickinson ME, Davis AR, Olmsted-Davis EA 2010 Vessel formation is induced prior to the appearance of cartilage in BMP-2-mediated heterotopic ossification. J Bone Miner Res **25**(5)**:**1147-56.
41. DeGrendele HC, Estess P, Picker LJ, Siegelman MH 1996 CD44 and its ligand hyaluronate mediate rolling under physiologic flow: a novel lymphocyte-endothelial cell primary adhesion pathway. J Exp Med **183**(3)**:**1119-30.
42. DeGrendele HC, Estess P, Siegelman MH 1997 Requirement for CD44 in activated T cell extravasation into an inflammatory site. Science **278**(5338)**:**672-5.
43. Gerber HP, Vu TH, Ryan AM, Kowalski J, Werb Z, Ferrara N 1999 VEGF couples hypertrophic cartilage remodeling, ossification and angiogenesis during endochondral bone formation. Nat Med **5**(6)**:**623-8.
44. Oberlin E, Amara A, Bachelerie F, Bessia C, Virelizier JL, Arenzana-Seisdedos F, Schwartz O, Heard JM, Clark-Lewis I, Legler DF, Loetscher M, Baggiolini M, Moser B 1996 The CXC chemokine SDF-1 is

the ligand for LESTR/fusin and prevents infection by T-cell-line-adapted HIV-1. Nature **382**(6594)**:**833-5.
45. Wagner DD, Frenette PS 2008 The vessel wall and its interactions. Blood **111**(11)**:**5271-81.
46. Decker B, Bartels H, Decker S 1995 Relationships between endothelial cells, pericytes, and osteoblasts during bone formation in the sheep femur following implantation of tricalciumphosphate-ceramic. Anat Rec **242**(3)**:**310-20.
47. Mishina Y, Snider TN 2014 Neural crest cell signaling pathways critical to cranial bone development and pathology. Exp Cell Res.
48. Garcia-Castro MI, Marcelle C, Bronner-Fraser M 2002 Ectodermal Wnt function as a neural crest inducer. Science **297**(5582)**:**848-51.
49. Lee HY, Kleber M, Hari L, Brault V, Suter U, Taketo MM, Kemler R, Sommer L 2004 Instructive role of Wnt/beta-catenin in sensory fate specification in neural crest stem cells. Science **303**(5660)**:**1020-3.
50. Kleber M, Lee HY, Wurdak H, Buchstaller J, Riccomagno MM, Ittner LM, Suter U, Epstein DJ, Sommer L 2005 Neural crest stem cell maintenance by combinatorial Wnt and BMP signaling. J Cell Biol **169**(2)**:**309-20.
51. Sullivan MP, Torres SJ, Mehta S, Ahn J 2013 Heterotopic ossification after central nervous system trauma: A current review. Bone Joint Res **2**(3)**:**51-7.
52. Shlosberg D, Benifla M, Kaufer D, Friedman A 2010 Blood-brain barrier breakdown as a therapeutic target in traumatic brain injury. Nat Rev Neurol **6**(7)**:**393-403.

Legends to Figures

Figure 1A. Osterix expression begins in the endoneurium of peripheral nerves. C57BL/6 mice (n=8) were injected with BMP2 producing cells 4 mice were euthanized at day 1 and 2. Frozen sections were prepared and immunostained for Neurofilament heavy chain (NF), CD31, or osterix. Colors are as indicated. DAPI is blue. H and E, sections were stained with hematoxylin and eosin.

Figure 1B. Expression of osterix, claudin 5, and CD31 at later times after BMP2 induction. C57BL/6 mice (n=16) were injected with BMP2 producing cells and 8 mice were euthanized at either day 4 or 7. Frozen sections were prepared and immunostained for CD31, claudin 5, or osterix as indicated. DAPI is blue.

Figure 1C. Osteoprogenitors for heterotopic ossification are not derived from de-differentiating Schwann cells. Osteoprogenitors in peripheral nerves were assessed at early (one day) and late (six days) after BMP2 induction by analyzing frozen serial sections of C57BL/6 mice (n=4 per group) euthanized 1 and 6 days after BMP2 induction. Sections were analyzed by immunohistochemistry for p75(NTR), osterix, and MPZ. Colors are as indicated.

Figure 2A. Cells expressing claudin 5 increase in blood after BMP2 induction. C57/BL6 mice (n=4 per group) either remained untreated or were injected with BMP2-producing cells. Mice were bled by cardiac puncture at 0 (untreated), 1, 2, and 4 days after induction. Mononuclear cells were collected, reacted with an antibody to claudin 5 and subjected to FACS. Descriptive statistics was used to analyze the study results. The sample size in the groups was n=3. The analysis of variance (ANOVA) with Bonferroni-Holm post-hoc correction for multiple comparisons was used to detect statistically-significant differences between the number of claudin 5^+ cells present in the circulation at given time points after intramuscular injection of BMP2-producing cells. The thresholds for statistically-significant differences were set at $p<0.05$.

Figure 2B. Claudin 5^+ circulating osteoprogenitors express osterix. Cells were isolated from muscle two days after BMP2 induction and claudin 5^+ and $^-$ cells isolated by preparative FACS. Each population was then subjected to cytospin and the resultant slides reacted with an antibody to osterix (red). Claudin 5, green; DAPI, blue. Claudin 5 positive population, A, B, and C; Claudin 5 negative population, E, F, and G).

Figure 3A. CD44, CXCR4, and E-selectin are expressed upon BMP2 induction. C57/BL6 mice were injected with BMP2-producing cells (n=8 per group) and at the times indicated mice were euthanized, RNA extracted from muscle around the site of injection, and the relative amount of RNA encoding **A)** CD44; **B)** CXCR4, and C) E-selectin was determined and comparisons to determine statistically significant differences

were made using an analysis of variance (ANOVA) with Bonferroni-Holm post-hoc correction for multiple comparisons. The thresholds for statistically-significant differences were set at $p<0.05$.

Figure 3B: Claudin 5^+ cells express CD44 and CXCR4 while claudin 5^- cells express E-selectin. C57BL/6 mice (n=4 per group) were injected with BMP2-producing cells and mice were euthanized four days later. Claudin 5^+ and claudin 5^- cells were isolated by preparative FACS,subjected to cytospin, and the resulting slides analyzed for staining for CD44, E-selectin, and CD44.

Figure 4. Claudin 5-positive cells express osteogenic markers. The claudin 5^+ population (green) was isolated from a FACS of cells isolated from muscle 4 days after BMP2 induction. These isolated cells were subjected to cytospin and the slides were then probed with antibodies for claudin 5 (green) and osterix (red). A, B, and C shows one field obtained from the claudin 5^+ population with C being the merger of A and B; D, E, and F show one field of the cytospin of a claudin 5^- population obtained from the same mouse that was stained with antibodies against claudin 5 (green) and osterix (red) as well as DAPI (F). In the claudin 5^+ cell population osterix positive cells were found to be 75% ± 3 %. In panels G-I and J-L, respectively, we show the cytospin patterns of the claudin 5 positive and negative populations of another mouse after staining for claudin 5 (green) and *dlx* 5 (red).

Figure 5A. Neural markers expressed in claudin 5 positive cells. C57BL/6 mice were either injected in the quadriceps with BMP2-producing cells or remained uninjected. After 4 days mice were euthanized and cells were isolated from the tissue around the site of injection, reacted with tagged antibodies against claudin 5 and PDGFRα and percentage of the total population positive for both markers was determined by FACS.
Figure 5B. Expression of musashi 1 in claudin 5 positive cells. C57BL/6 mice were either injected in the quadriceps with BMP2-producing cells, A-F or remained uninjected, G-L. After 4 days the mice were euthanized and cells from muscle around the site of injection were isolated, reacted with an antibody against claudin 5 tagged with Alexa fluor 488 (green) and subjected to FACS. The claudin 5 positive (A-C and G-I) and claudin 5 negative (D-F and J-L) populations were isolated from both the BMP2-induced as well as uninjected mice, subjected to cytospin and the resultant slides stained with DAPI (blue) and an antibody to musashi 1 (red).

Figure 6 A. Osteoprogenitors express the endothelial marker Tie 2. C57/BL6 mice were injected with BMP2-producing cells (n=4) and four days after induction the mice were euthanized and cells harvested from the muscle around the site of injection were separated by FACS into claudin 5 positive and negative populations. The populations were subjected to cytospin and the slides were assessed for expression of Tie2 (red). Claudin 5, green; DAPI, blue. **B.** This is a representative photomicrograph 40X magnification showing an asymmetric distribution of Tie-2 (red) in some of the cells.

Figure 1A

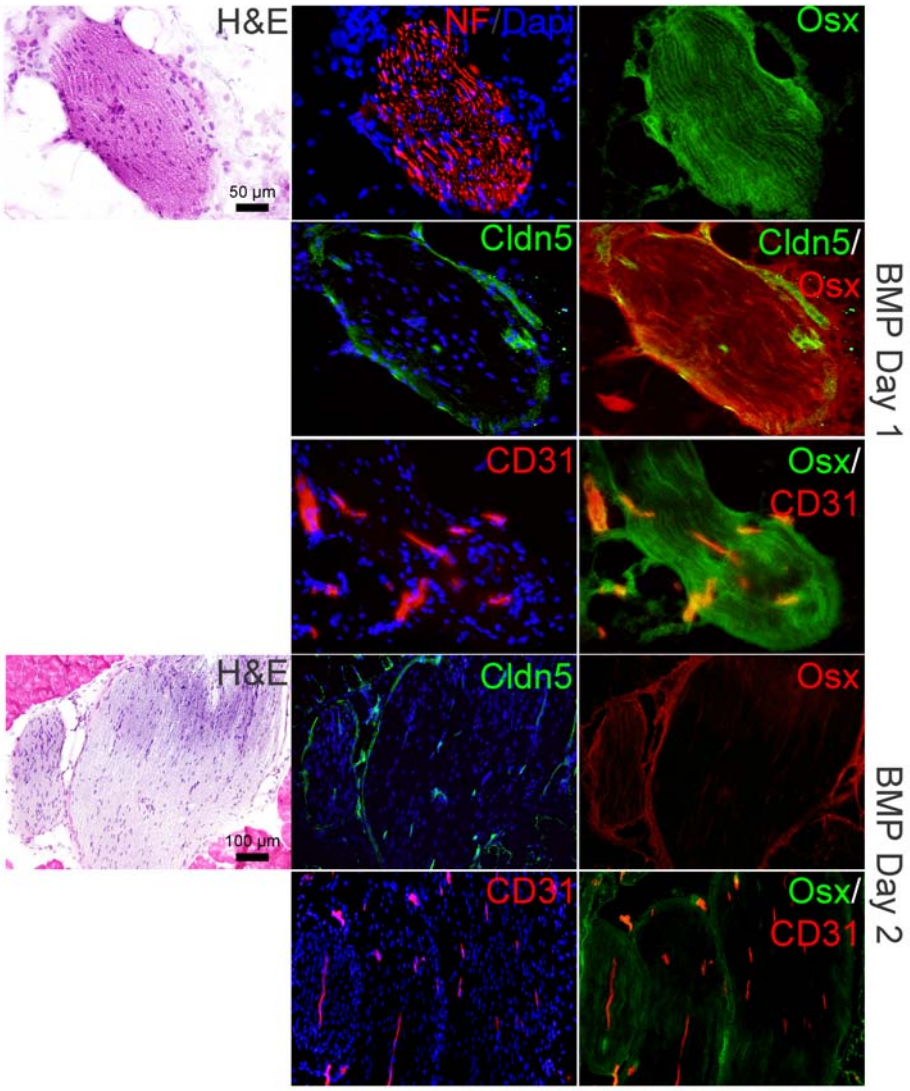
H&E
NF/Dapi
Osx
50 µm
Cldn5
Cldn5/
Osx
BMP Day 1
CD31
Osx/
CD31
H&E
Cldn5
Osx
100 µm
BMP Day 2
CD31
Osx/
CD31

Figure 1B

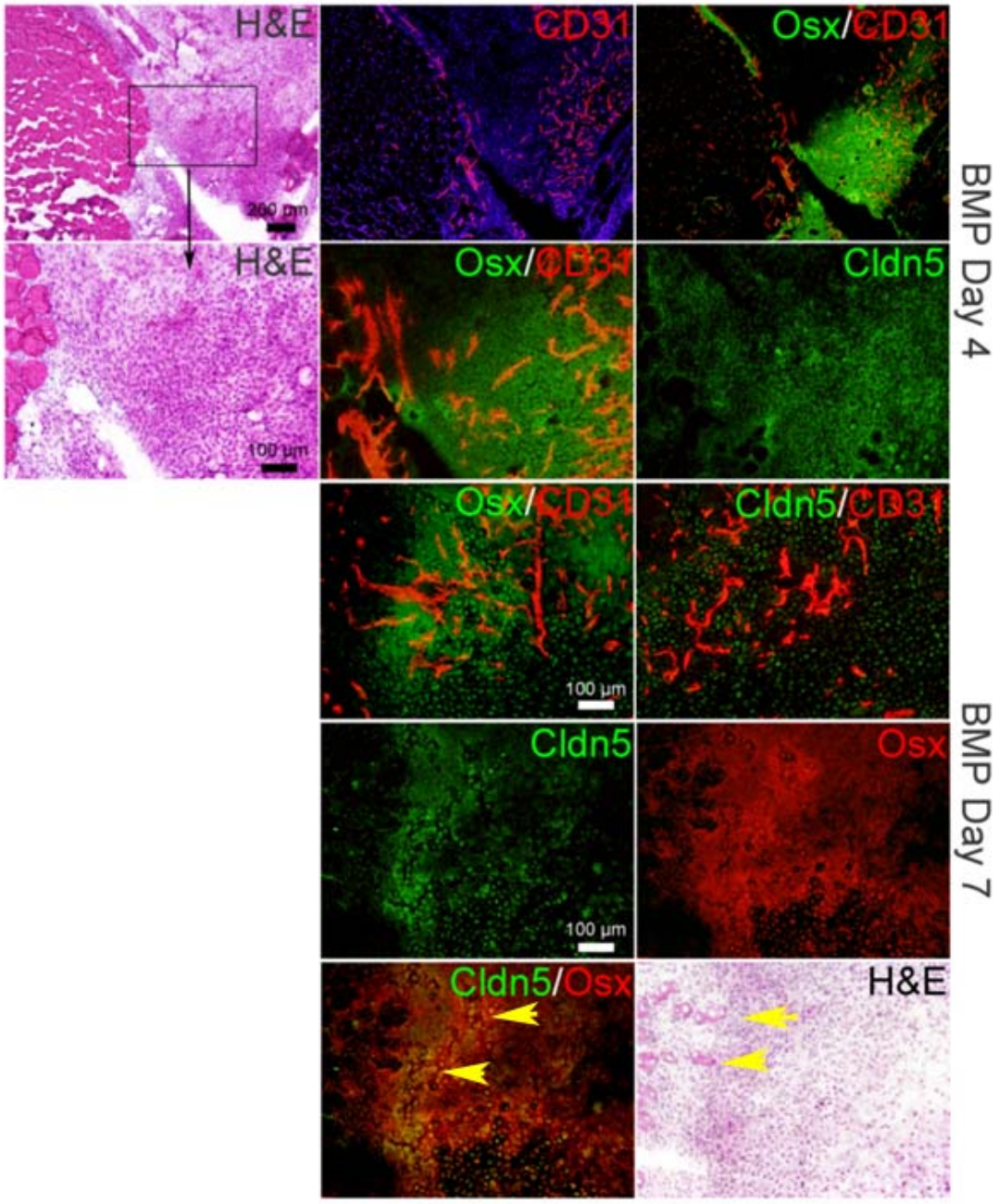
H&E
CD31
Osx/CD31
200 μm
H&E
Osx/CD31
Cldn5
100 μm
BMP Day 4
Osx/CD31
Cldn5/CD31
100 μm
Cldn5
Osx
100 μm
BMP Day 7
Cldn5/Osx
H&E

Figure 1C

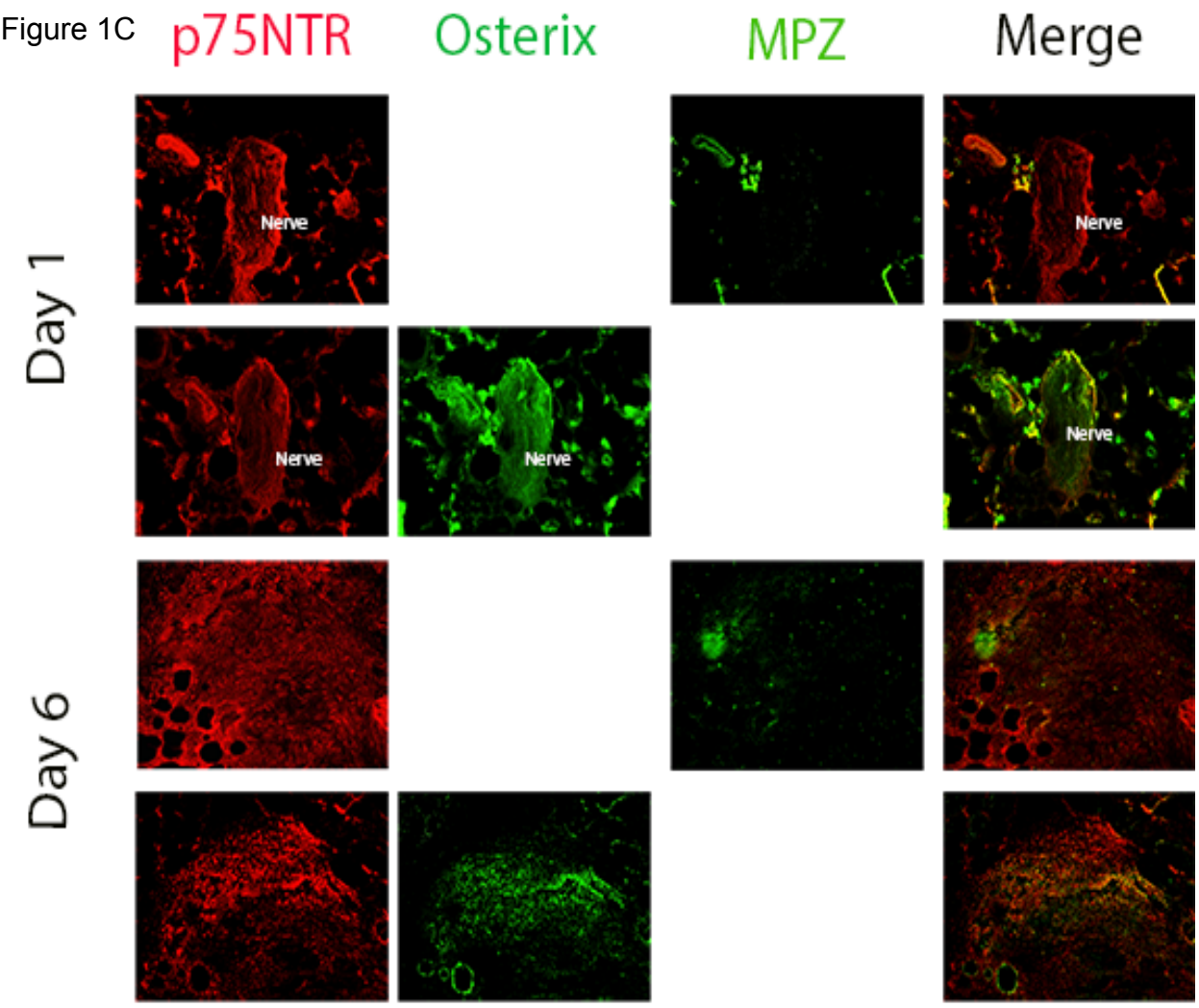
p75NTR
Osterix
MPZ
Merge
Day 1
Day 6
Nerve
Nerve
Nerve
Nerve
Nerve

Figure 2A

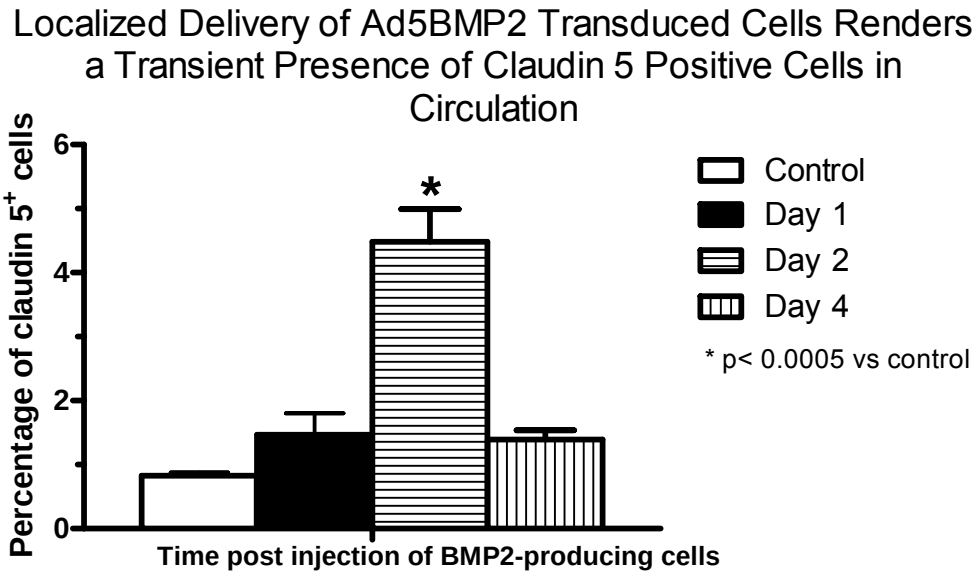

Figure 2B

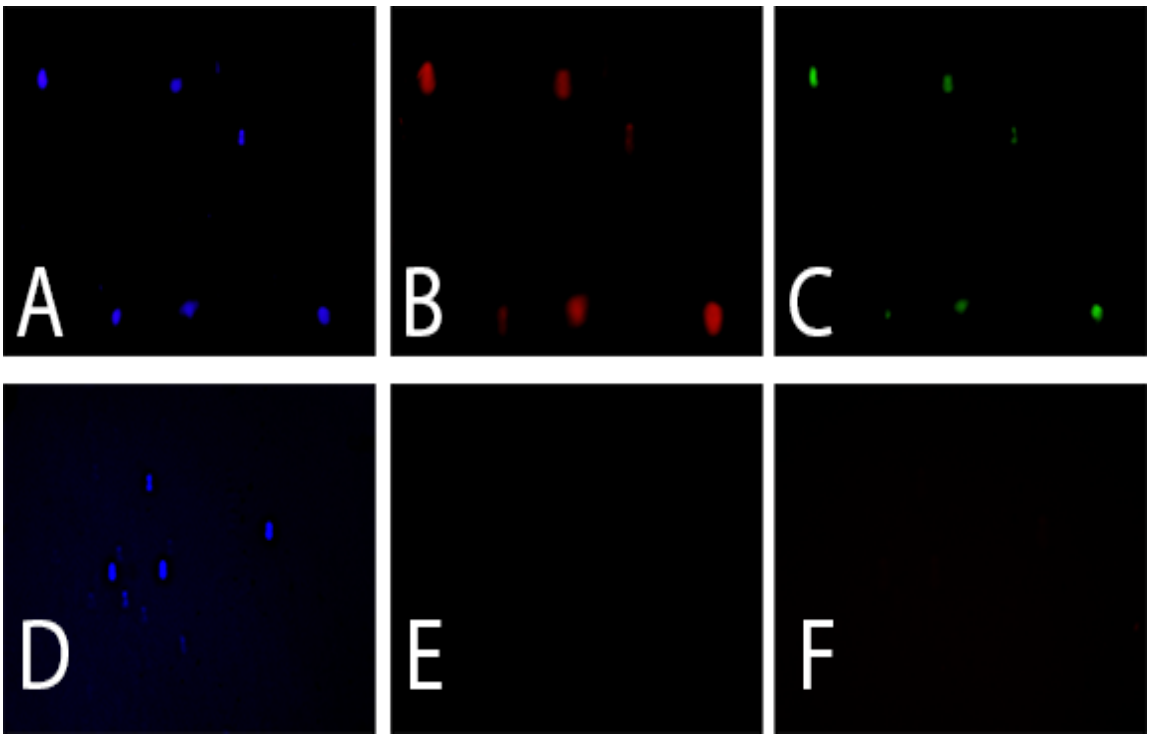

Figure 3A

Figure 3B

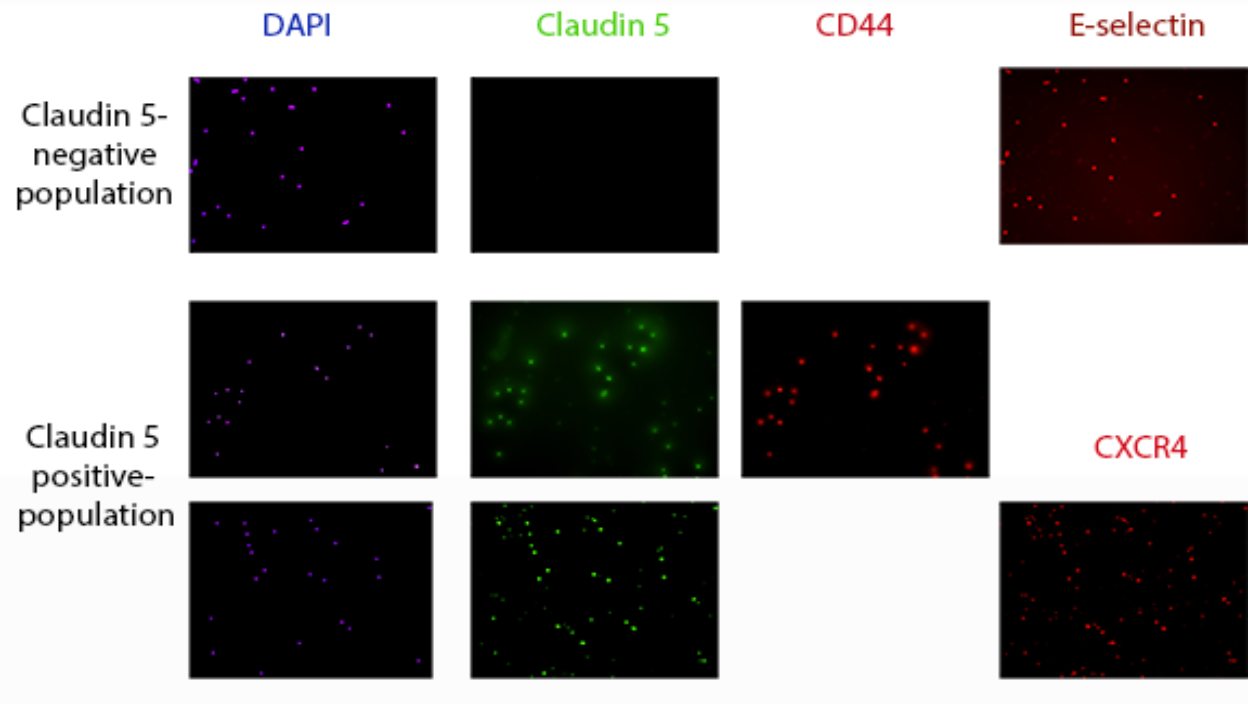
DAPI
Claudin 5
CD44
E-selectin
Claudin 5-negative population
Claudin 5 positive-population
CXCR4

Figure 4.

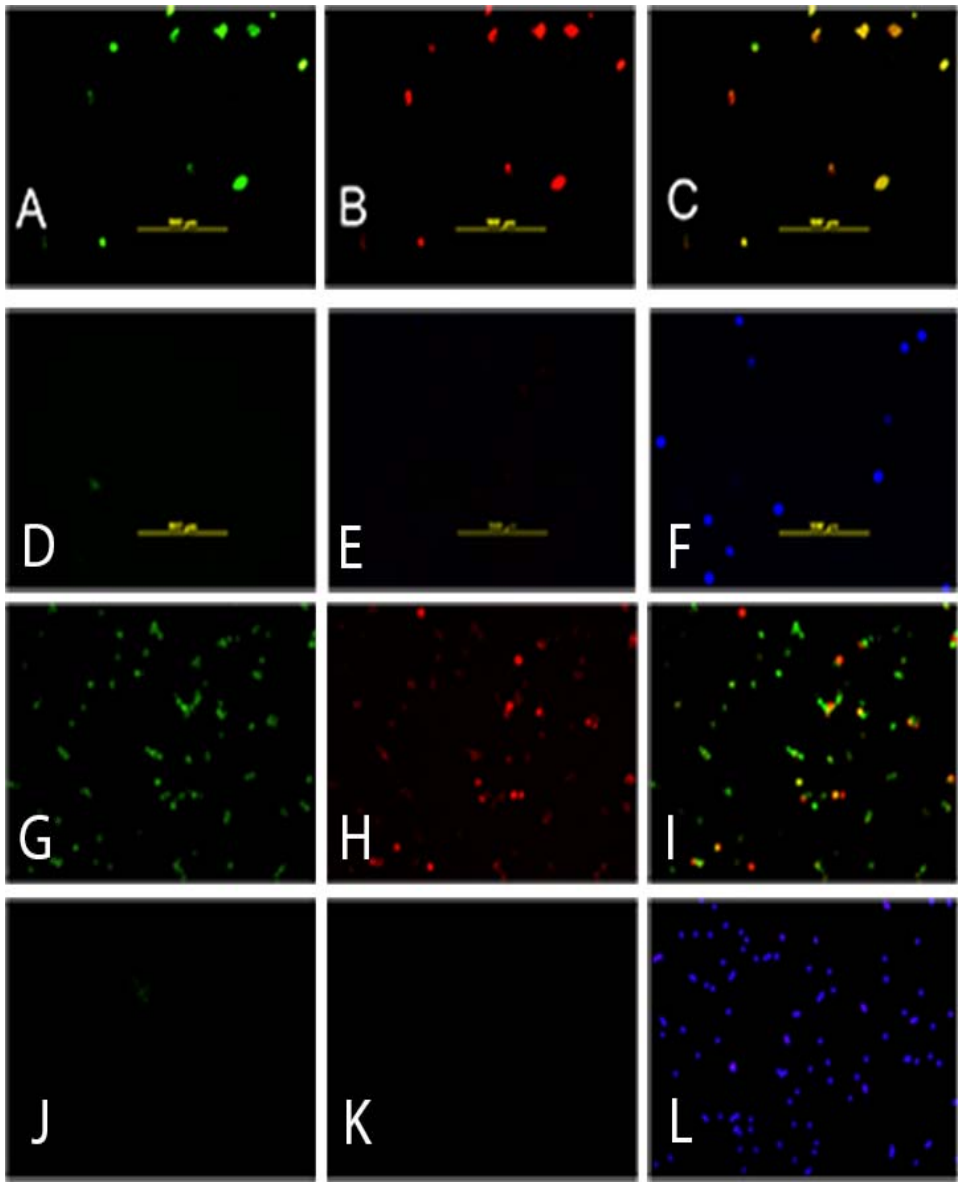

Figure 5A.

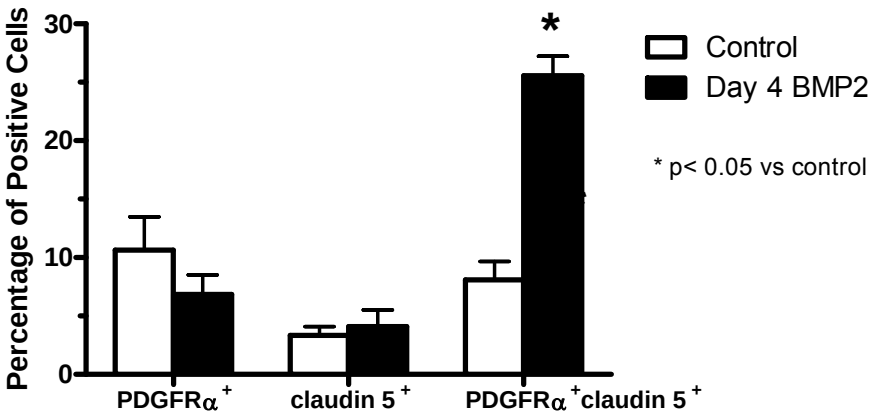

Figure 5B

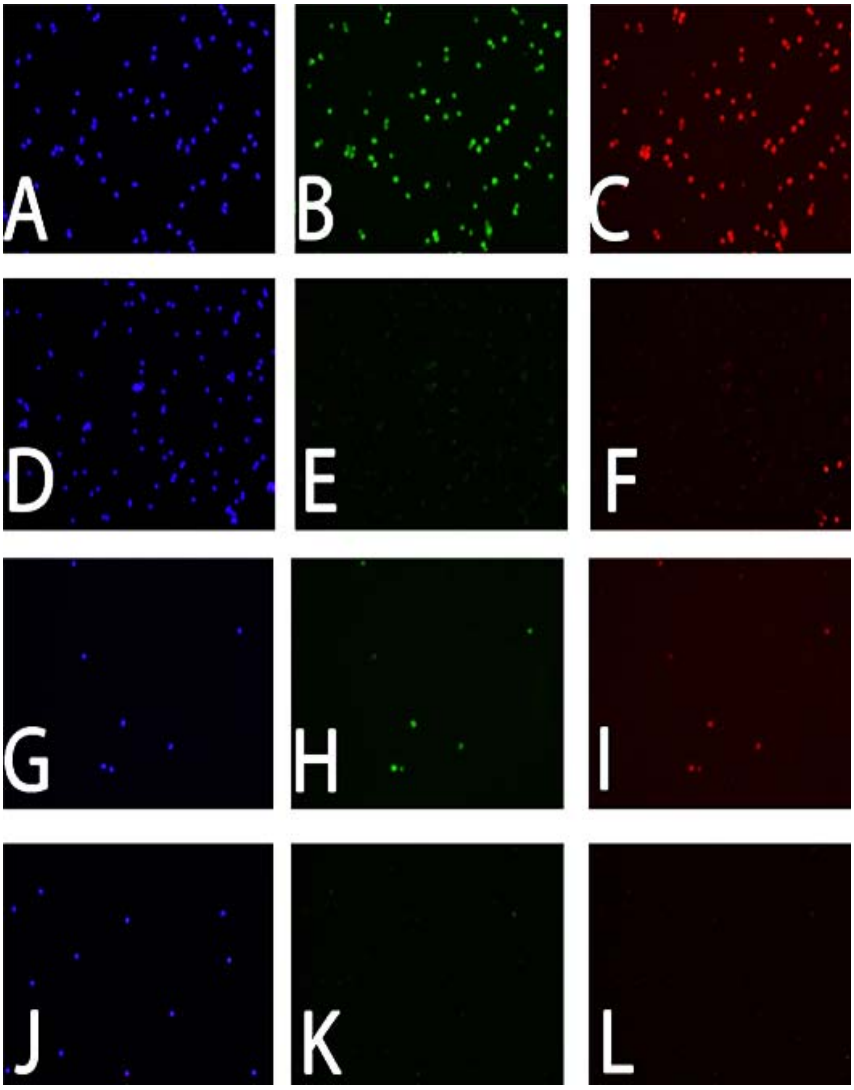

Figure 6A

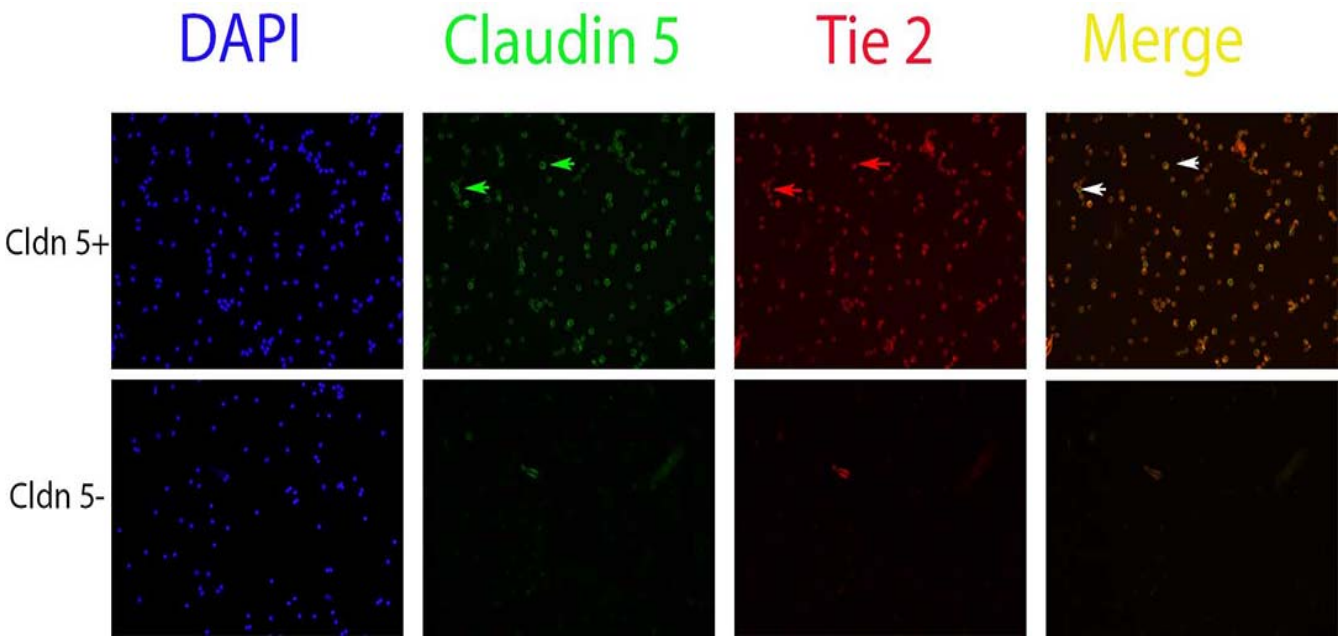

Figure 6B